CERN-PH-EP/2012-273
2012/10/01

CMS-SUS-12-006

Search for electroweak production of charginos and neutralinos using leptonic final states in pp collisions at $\sqrt{s} = 7 \text{ TeV}$

The CMS Collaboration*

Abstract

The 2011 dataset of the CMS experiment, consisting of an integrated luminosity of 4.98 fb^{-1} of pp collisions at $\sqrt{s} = 7 \text{ TeV}$, enables expanded searches for direct electroweak pair production of charginos and neutralinos in supersymmetric models as well as their analogs in other models of new physics. Searches sensitive to such processes, with decays to final states that contain two or more leptons, are presented. Final states with three leptons, with a same-sign lepton pair, and with an opposite-sign lepton pair in conjunction with two jets, are examined. No excesses above the standard model expectations are observed. The results are used in conjunction with previous results on four-lepton final states to exclude a range of chargino and neutralino masses from approximately 200 to 500 GeV in the context of models that assume large branching fractions of charginos and neutralinos to leptons and vector bosons.

Submitted to the Journal of High Energy Physics

*See Appendix B for the list of collaboration members

1 Introduction

Many searches for physics beyond the standard model (BSM) performed by experiments at the CERN Large Hadron Collider (LHC) have focused on models with cross sections dominated by the production of new heavy strongly interacting particles, with final states characterized by large hadronic activity. These searches are well justified since strongly interacting particles can be produced with large cross sections and hence be observable with early LHC data. In the context of supersymmetry (SUSY) [1–7], such models lead mainly to the production of the strongly interacting squarks and gluinos, the SUSY partners of the quarks and gluons. In contrast, in this paper we describe searches for BSM physics dominated by the direct electroweak production of particles that might not yield large hadronic activity, and that may therefore have eluded detection in early searches. This signature characterizes SUSY models with pair-production of electroweak charginos $\tilde{\chi}^\pm$ and neutralinos $\tilde{\chi}^0$, mixtures of the SUSY partners of the gauge bosons and Higgs bosons. Depending on the mass spectrum, the charginos and neutralinos can have significant decay branching fractions (BF) to leptons or vector bosons, resulting in final states that contain either on-shell vector bosons or three-lepton states with continuous pair-mass distributions [8–13]. In either case, neutrino(s) and two stable lightest-SUSY-particle (LSP) dark-matter candidates are produced, which escape without detection and lead to large missing transverse energy E_T^{miss} in the event.

In this paper, we present several dedicated searches for chargino-neutralino pair production. The data, corresponding to an integrated luminosity of $4.98 \pm 0.11 \text{ fb}^{-1}$ [14] of proton-proton collisions at $\sqrt{s} = 7 \text{ TeV}$, were collected by the Compact Muon Solenoid (CMS) experiment at the LHC in 2011. Even with the smaller cross sections of electroweak production, this data sample is sufficient to probe the production of charginos and neutralinos with masses well beyond existing constraints [15–22]. Since LHC studies have as yet found no evidence for new strongly interacting particles, we focus on scenarios in which such particles do not participate, and in which the final states are rich in leptons produced via intermediate states including sleptons (SUSY partners of the leptons, including sneutrinos, partners of neutrinos). These scenarios include cases such as those shown in Figs. 1 and 2, which are labeled using SUSY nomenclature, though the interpretation naturally extends to other BSM models. In the SUSY nomenclature, $\tilde{\chi}_1^0$ is the lightest neutralino, presumed to be the LSP, and $\tilde{\chi}_2^0$ and $\tilde{\chi}_3^0$ are heavier neutralinos; $\tilde{\chi}_1^\pm$ is the lightest chargino. In Fig. 1 the slepton mass $m_{\tilde{\ell}}$ is less than the masses $m_{\tilde{\chi}_2^0}$ and $m_{\tilde{\chi}_1^\pm}$, while in Fig. 2 it is greater, and the mass difference between the LSP and the next-lightest chargino or neutralino is large enough to lead to on-shell vector bosons. In addition to the dedicated searches, we leverage the results of some previous CMS SUSY searches [23–26], either by interpreting the previous results directly in the context of the scenarios in Figs. 1 and 2, or by modifying the previous studies so that they target electroweak, rather than strong, production processes. Throughout this paper, “lepton” refers to a charged lepton; in specified contexts, it refers more specifically to an experimentally identified electron or muon.

To quantify our results, we present them in the context of simplified model spectra (SMS) [27–34]. SUSY models with bino-like $\tilde{\chi}_1^0$ and wino-like $\tilde{\chi}_2^0$ and $\tilde{\chi}_1^\pm$ lead to the SMS trilepton signature of Fig. 1, and motivate the simplifying assumption that the latter two gauginos have similar masses as a result of belonging to the same gauge group multiplet. We thus set $m_{\tilde{\chi}_2^0} = m_{\tilde{\chi}_1^\pm}$, and present results as a function of this common mass and the LSP mass $m_{\tilde{\chi}_1^0}$. The results for Fig. 1 depend also on the mass $m_{\tilde{\ell}}$ of the intermediate slepton (if left-handed, taken to be the same for its sneutrino $\tilde{\nu}$), parametrized in terms of a variable $x_{\tilde{\ell}}$ as

$$m_{\tilde{\ell}} = m_{\tilde{\chi}_1^0} + x_{\tilde{\ell}} (m_{\tilde{\chi}_1^\pm} - m_{\tilde{\chi}_1^0}), \quad (1)$$

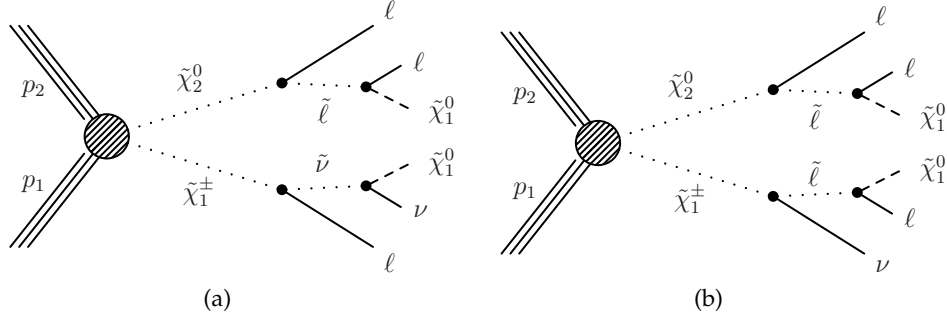


Figure 1: Diagrams of chargino-neutralino pair production in proton-proton collisions followed by decays leading to a final state with three leptons, two LSPs, and a neutrino. For left-handed sleptons (with accompanying sneutrinos), both diagrams exist, and for each diagram there is an additional diagram with $\tilde{\chi}_2^0 \rightarrow \ell \tilde{\ell} \rightarrow \ell \ell \tilde{\chi}_1^0$ replaced by $\tilde{\chi}_2^0 \rightarrow \tilde{\nu} \nu \rightarrow \nu \nu \tilde{\chi}_1^0$. Thus only 50% of produced pairs results in three leptons. For right-handed sleptons, only the right diagram exists, and 100% of produced pairs result in three leptons. In these diagrams and those of Fig. 2, dotted lines represent unstable intermediate states, and the dashed lines represent the LSP.

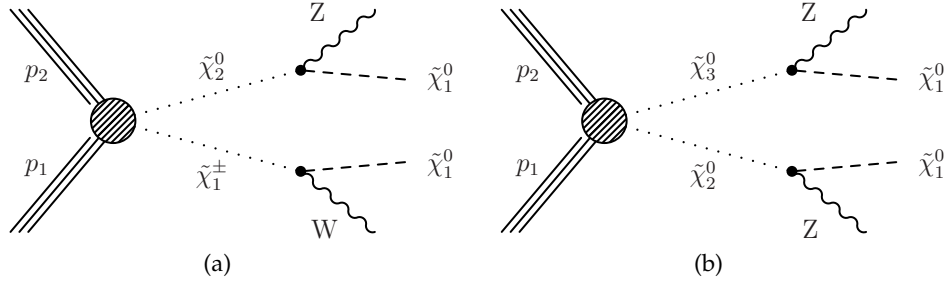


Figure 2: Diagrams of chargino-neutralino and neutralino-neutralino pair production in proton-proton collisions followed by decay to on-shell W or Z bosons and LSPs.

where $0 < x_{\tilde{\ell}} < 1$. We present results for $x_{\tilde{\ell}}$ equal to 0.5 (i.e., the slepton mass equal to the mean of the LSP and chargino masses). In some cases we also present results for $x_{\tilde{\ell}} = 0.25$ and 0.75.

The interpretation of the result may further depend on whether the sleptons are the SUSY partner $\tilde{\ell}_L$ or $\tilde{\ell}_R$ of left-handed or right-handed leptons. We consider two limiting cases. In one case, $\tilde{\ell}_R$ does not participate while $\tilde{\ell}_L$ and $\tilde{\nu}$ do: then both diagrams of Fig. 1 exist, and the chargino and neutralino decay to all three lepton flavors with equal probability. Furthermore, two additional diagrams with $\tilde{\chi}_2^0 \rightarrow \ell \tilde{\ell} \rightarrow \ell \ell \tilde{\chi}_1^0$ replaced by $\tilde{\chi}_2^0 \rightarrow \tilde{\nu} \nu \rightarrow \nu \nu \tilde{\chi}_1^0$ reduce the fraction of three-lepton final states by 50%. In the second case, in which $\tilde{\ell}_R$ participates while $\tilde{\ell}_L$ and $\tilde{\nu}$ do not, only the diagram of Fig. 1(b) exists, and there is no 50% loss of three-lepton final states. Because the $\tilde{\ell}_R$ couples to the chargino via its higgsino component, chargino decays to $\tilde{\ell}_R$ strongly favor the τ as the lepton. For the leptonic decay products, we thus consider primarily two flavor scenarios:

- The “flavor-democratic” scenario: the chargino ($\tilde{\chi}_1^\pm$) and neutralino ($\tilde{\chi}_2^0$) both decay with equal probability into all three lepton flavors, as expected for $\tilde{\ell}_L$;
- The “ τ -enriched” scenario: the chargino decays exclusively to τ leptons as expected

for $\tilde{\ell}_R$, while the neutralino decays democratically.

With the selection criteria used in this paper, we have only limited sensitivity to a third scenario: the “ τ -dominated” scenario in which the chargino and neutralino both decay only to a τ lepton.

We place limits on the pair production cross section times branching fraction in the above scenarios. In additional interpretations given below in terms of bounds on masses within SMS, the 50% branching fraction to three leptons is taken into account when appropriate in $\tilde{\ell}_L$ cases. For $x_{\tilde{\ell}} = 0.5$, the kinematic conditions for the processes of Fig. 1 are identical for $\tilde{\ell}_L$ and $\tilde{\ell}_R$, and the respective limits are trivially related. For other values of $x_{\tilde{\ell}}$ (0.25 and 0.75), differences in experimental acceptance may alter the relationship.

For results based on the diagrams of Fig. 2, we assume that sleptons are too massive to participate, so that the branching fractions to vector bosons are 100%. Even with such an assumption, there is little sensitivity to the ZZ channel of Fig. 2(b) in the context of models such as the minimal supersymmetric extension of the standard model (MSSM), where neutralino pair production is suppressed relative to neutralino-chargino production. Rather, for the ZZ signature, we consider a specific gauge-mediated supersymmetry breaking (GMSB) Z-enriched higgsino model [35–37] that enhances the $ZZ + E_T^{\text{miss}}$ final state.

Following a description of the data collection and reconstruction procedures in Section 2, Section 3 describes searches specifically aimed at the three-lepton final state of Fig. 1. Kinematic observables that can distinguish signal from background include [38–41] E_T^{miss} , the invariant mass $M_{\ell\ell}$ of the opposite-sign leptons, and the transverse mass M_T formed from one lepton and the E_T^{miss} . A three-lepton search using E_T^{miss} is presented in Section 3.1, while a complementary approach using $M_{\ell\ell}$ and M_T is presented in Section 3.2. In these three-lepton searches, the leptons selected are electrons and muons. Sensitivity to τ leptons arises only through their leptonic decays.

The three-lepton searches lose sensitivity when the probability to detect the third lepton becomes low. In Section 4, we describe a search based on exactly two reconstructed leptons with the same electric charge (same sign), which extends the sensitivity to the processes of Fig. 1. This study, a modification of the CMS search for SUSY described in Ref. [26], includes hadronically decaying τ leptons in addition to electrons and muons. Section 5 describes a search for the on-shell W and Z boson production processes of Fig. 2. This study is a modification of the CMS search for SUSY in the Z boson plus jets and E_T^{miss} channel [25].

Section 6 presents an interpretation of these searches, in some cases combining several together, and including the four-lepton results of Ref. [24]. Results of related searches have also been recently reported by the ATLAS collaboration [42, 43].

Finally, Appendix A provides a parametrized function for the detection efficiency of physics objects used in the analysis in Section 3.2. This function will enable estimation of sensitivities for BSM models not considered in this paper that yield three leptons in the final state.

2 Detector, online selection, and object selection

The online event selections (trigger) and further offline object selections closely follow those described in Ref. [24], and are briefly summarized here. Exceptions are noted below in the sections specific to each analysis.

The central feature of the CMS apparatus is a superconducting solenoid, of 6 m internal diameter, providing a magnetic field of 3.8 T. Within the field volume are a silicon pixel and strip

tracker, a crystal electromagnetic calorimeter (ECAL), and a brass/scintillator hadron calorimeter. Muons are measured in gas-ionization detectors embedded in the steel return yoke. Extensive forward calorimetry complements the coverage provided by the barrel and endcap detectors. A more detailed description can be found in Ref. [44].

CMS uses a right-handed coordinate system, with the origin at the nominal interaction point, the x axis pointing to the center of the LHC, the y axis pointing upwards (perpendicular to the plane of the LHC ring), and the z axis along the counterclockwise-beam direction. The polar angle θ is measured from the positive z axis, and the azimuthal angle ϕ (in radians) is measured in the x - y plane. The pseudorapidity η is a transformation of the polar angle defined by $\eta = -\ln[\tan(\theta/2)]$.

Events from pp interactions must satisfy the requirements of a two-level trigger system. The first level performs a fast selection for physics objects (jets, muons, electrons, and photons) above certain thresholds. The second level performs a full event reconstruction. Events in this analysis are primarily selected using double-lepton triggers that require at least one electron or muon with transverse momentum $p_T > 17$ GeV, and another with $p_T > 8$ GeV, with $|\eta| < 2.5$ for electrons and $|\eta| < 2.4$ for muons. For channels involving τ leptons, triggers are used that rely on significant hadronic activity and E_T^{miss} , in addition to the presence of a single lepton or two hadronic τ candidates [26]. Additional triggers are used for calibration and efficiency studies.

Simulated event samples are used to study the characteristics of signal and standard model (SM) background. Most of the simulated event samples are produced with the MADGRAPH 5.1.1 [45, 46] event generator, with parton showering and hadronization performed with the PYTHIA 8.1 [47] program. Signal samples are generated with PYTHIA 6.424 [47]. The samples are generated using the CTEQ 6L1 [48] parton distribution functions. For the diboson backgrounds, MCFM [49] samples are used to help assess the theoretical uncertainties on the simulated samples. For the simulated SM samples, we use the most accurate calculations of the cross sections available, generally with next-to-leading order (NLO) accuracy [50–52]. The files specifying the SUSY signal model parameters are generated according to the SUSY Les Houches accord [53] standards with the ISAJET program [54], with cross sections calculated in PYTHIA to leading order and NLO corrections calculated using PROSPINO 2.1 [55]. Depending on the simulated sample, the detector response and reconstruction are modeled either with the CMS fast simulation framework [56], or with the GEANT4 [57] program, followed by the same event reconstruction as that used for data.

Events are reconstructed offline using the particle-flow (PF) algorithm [58, 59], which provides a self-consistent global assignment of momenta and energies. Details of the reconstruction and identification are given in Refs. [60, 61] for electrons and muons. Leptonically decaying τ leptons are included in the selection of electrons or muons. In the same-sign dilepton search, hadronic τ lepton decays are identified with the “hadrons-plus-strips” algorithm [26, 62]. This algorithm combines PF photons and electrons into strips (caused by azimuthal bending of an electromagnetic shower in the CMS magnetic field) in order to reconstruct neutral pions. The neutral pions are combined with charged hadrons to reconstruct exclusive hadronic τ decay topologies. In the four-lepton results from Ref. [24] used in the interpretations in Section 6, hadronic τ candidates are identified as isolated tracks with associated ECAL energy deposits consistent with those from neutral pions.

We consider events that contain electrons, muons, and (for a subset of the searches, as specified above) hadronically decaying τ leptons, each associated with the same primary vertex. Offline requirements on the lepton p_T and η are described in the analysis-specific sections below. To

reduce contamination due to leptons from heavy-flavor decays or misidentified hadrons in jets, an isolation criterion is formed by summing the track p_T and calorimeter E_T values in a cone of $\Delta R = 0.3$ (0.4 for electrons in the three-lepton+ E_T^{miss} search) around the lepton, where $\Delta R = \sqrt{(\Delta\phi)^2 + (\Delta\eta)^2}$. The candidate lepton is excluded from the isolation sum. This sum is divided by the lepton's p_T to obtain the isolation ratio I_{rel} , which is required to be less than 0.15.

Jets are reconstructed with the anti- k_T clustering algorithm [63] with a distance parameter of 0.5. The jet reconstruction is based on PF objects. With exceptions noted below, jets are required to have $|\eta| < 2.5$ and $p_T > 40$ GeV and to be separated from any lepton satisfying the analysis selection by $\Delta R > 0.3$. Where applicable to suppress background from heavy flavors, we identify jets with b quarks (referred to throughout as “b jets”) by using the CMS “track-counting high-efficiency algorithm” (TCHE) [64], which provides a b-jet tagging efficiency of 76% (63%) with a misidentification rate of 13% (2%) for the loose (medium) working point.

Events with an opposite-sign same-flavor (OSSF) dilepton (i.e., dielectron or dimuon) with invariant mass below 12 GeV are rejected, to exclude quarkonia resonances, low-mass continuum, and photon conversions.

3 Searches in the three-lepton final state

For the searches in the three-lepton final state, we use reconstructed leptons identified as electrons and muons; any sensitivity to τ leptons comes indirectly through their leptonic decays. The main SM backgrounds in the three-lepton final state are from WZ production with three genuine isolated leptons that are “prompt” (created at the primary vertex), and from $t\bar{t}$ production with two such leptons and a third particle identified as such but that is “non-prompt” (created at a secondary vertex, as from a heavy-flavor decay) or not a lepton. We consider two complementary variants of this search. The first uses the missing transverse energy E_T^{miss} directly, and has slightly better sensitivity than the second when the difference between $m_{\tilde{\chi}_2^0} = m_{\tilde{\chi}_1^\pm}$ and the LSP mass $m_{\tilde{\chi}_1^0}$ is large. The second search uses E_T^{miss} indirectly through the transverse mass M_T , which is particularly effective in discriminating background from leptonic decays of W bosons in events with lower E_T^{miss} ; this search has more sensitivity than the first as $m_{\tilde{\chi}_1^0}$ approaches $m_{\tilde{\chi}_2^0} = m_{\tilde{\chi}_1^\pm}$.

3.1 Searches with three leptons using E_T^{miss} shape

For our study of three-lepton events with significant E_T^{miss} , we make use of our previous analysis [24], based on the same data sample as the present study. The analysis requires three leptons (only electrons or muons) and $H_T < 200$ GeV, where H_T is the scalar sum of the p_T of the jets in the event. OSSF dileptons are rejected if $75 \text{ GeV} < M_{\ell\ell} < 105 \text{ GeV}$ in order to suppress background from Z bosons. For the lepton selection, at least one electron or muon is required with $p_T > 20$ GeV, and another with $p_T > 10$ GeV; the third lepton must have $p_T > 8$ GeV; this search additionally requires $|\eta| < 2.1$ for all three leptons. A more detailed description of the analysis can be found in Ref. [24].

The number of events observed for $E_T^{\text{miss}} > 50$ GeV and the corresponding background predictions are given in Table 1 in 10-GeV-wide bins (corresponding to the display of the same data in Fig. 3 (left) of Ref. [24]). The analysis in Ref. [24] considers two regions of E_T^{miss} only: $E_T^{\text{miss}} < 50$ GeV and $E_T^{\text{miss}} > 50$ GeV. In the present study, we take this latter region and use the separate contents of the bins in Table 1 in a combined statistical treatment. This approach

provides more powerful discrimination between signal and background than the treatment of Ref. [24], because of the different shapes of signal and background across these bins.

All details of the event selection, background estimates, and evaluation of systematic uncertainties are as described in Section 2 and Ref. [24]. Briefly, efficiencies of electron/muon identification and isolation requirements are estimated using the method described in Ref. [65] for $Z \rightarrow \ell^+\ell^-$ events, and are in agreement with the simulation to within 2% (1%) for electrons (muons). Background due to Drell-Yan processes (including $Z + \text{jets}$ boson production), with a jet providing a third genuine (non-prompt) lepton or a hadron misidentified as a lepton, is evaluated from studies of isolated tracks failing or passing electron/muon identification criteria, separately for samples enriched in heavy- and light-flavor jets. This background decreases rapidly to negligible levels for $E_T^{\text{miss}} > 50$ GeV. The main backgrounds for $E_T^{\text{miss}} > 50$ GeV are from diboson and $t\bar{t}$ production and are estimated from the simulation.

Table 1: The observed and mean expected background in bins of E_T^{miss} for three-lepton events with $H_T < 200$ GeV, an opposite-sign same-flavor (OSSF) lepton pair, and no Z boson candidate. These results correspond to the distributions shown in Fig. 3 (left) of Ref. [24]. Uncertainties include statistical and systematic contributions.

E_T^{miss} Range (GeV)	Observation	Background
50-60	5	7.01 ± 2.15
60-70	10	5.36 ± 1.46
70-80	2	3.35 ± 0.93
80-90	5	2.52 ± 0.68
90-100	1	2.14 ± 0.56
100-110	0	2.37 ± 0.83
110-120	3	1.49 ± 0.47
120-130	1	1.06 ± 0.32
130-140	0	0.38 ± 0.11
140-150	2	0.26 ± 0.10
150-160	0	0.15 ± 0.06
160-170	1	0.16 ± 0.06
170-180	0	0.08 ± 0.03
180-190	0	0.54 ± 0.42
190-200	0	0.05 ± 0.03
>200	0	0.33 ± 0.16

Section 6 presents the detailed interpretation of these results.

3.2 Searches with three leptons using $M_{\ell\ell}$ and M_T

The alternative three-lepton search, based on $M_{\ell\ell}$ and M_T , introduces in addition a veto on events having an identified b jet (using the TCHE medium working point) with $p_T > 20$ GeV. By vetoing only b jets, this requirement suppresses $t\bar{t}$ background while avoiding exposure to signal loss (for example due to initial-state radiation) from a more general jet veto.

We require at least one electron or muon with $p_T > 20$ GeV and two more with $p_T > 10$ GeV, all with $|\eta| < 2.4$. After requiring $E_T^{\text{miss}} > 50$ GeV (and making no requirement on H_T), events are characterized by the values of the invariant mass $M_{\ell\ell}$ of the OSSF pair, and the transverse mass M_T formed from the E_T^{miss} vector and the transverse momentum p_T^ℓ of the remaining lepton:

$$M_T \equiv \sqrt{2E_T^{\text{miss}} p_T^\ell [1 - \cos(\Delta\phi_{\ell, E_T^{\text{miss}}})]}. \quad (2)$$

For three-muon and three-electron events, the OSSF pair with $M_{\ell\ell}$ closer to the Z mass is used. For backgrounds where a true OSSF pair arises from a low-mass virtual photon, this can result in a misassignment; simulation of this effect is validated with identified $\mu\mu e$ and μee events by treating all three leptons as having the same flavor.

3.2.1 Background due to WZ production

The largest background is due to SM WZ production in which both bosons decay leptonically. Studies with data indicate that the simulation-based estimates of systematic uncertainties on both the WZ background characteristics and signal resolutions are generally reliable, but especially at high- M_T , corrections are obtainable through detailed comparisons of data and the simulation. Here, we present one such study: the calibration of the hadronic recoil of the WZ system. In addition, the overall WZ event yield normalization is validated using events where $M_{\ell\ell}$ and M_T are consistent with the Z and W boson masses ($81 \text{ GeV} < M_{\ell\ell} < 101 \text{ GeV}$, $M_T < 100 \text{ GeV}$), respectively. We find good agreement with the SM simulations, as presented below.

The simulation of E_T^{miss} (and hence M_T) is corrected using a generalization of the Z-recoil method used in the CMS measurements of the W and Z cross sections [65]. The transverse hadronic recoil vector \vec{u}_T is

$$\vec{u}_T = -\vec{E}_T^{\text{miss}} - \vec{p}_{T,1} - \vec{p}_{T,2} \quad (3)$$

for Z events and

$$\vec{u}_T = -\vec{E}_T^{\text{miss}} - \vec{p}_{T,1} - \vec{p}_{T,2} - \vec{p}_{T,3} \quad (4)$$

for WZ events, where \vec{E}_T^{miss} is the missing transverse energy vector, and $\vec{p}_{T,i}$ is the transverse momentum vector of each of the two leptons from the Z decay or three leptons from the WZ decay. The recoil vector is resolved into components: u_1 parallel to the direction of the respective Z or WZ system, and u_2 perpendicular to the Z or WZ direction (known in the simulation and approximated in the data). The u_1 component is sensitive to calorimeter response and resolution, while the u_2 component is predominantly determined by the underlying event and multiple interactions. Using a pure sample of Z boson events, detailed studies of both components as a function of the Z boson p_T value yield corrections to the simulation, which are implemented event-by-event assuming that the results for Z production are similar to those for WZ production. These data-based corrections alter the expected background by up to 25%, and allow us to reduce the systematic uncertainty associated with the simulation.

Reconstructed leptonic decays of Z bosons are used to calibrate lepton energy scales and resolutions, separately for electrons and muons, in bins of p_T and η . The uncertainties from this procedure are propagated into uncertainties on the mean background estimation by using the simulation. Table 2 summarizes these and the other systematic uncertainties in the estimation of the WZ background.

3.2.2 Background due to $t\bar{t}$ production and other processes

The second-largest background is from events with two genuine isolated prompt leptons and a third identified lepton that is either a non-prompt genuine lepton from a heavy-flavor decay or a misidentified hadron, typically from a light-flavor jet. Top-quark pair, Z + jets, and WW + jets events are the main processes that contribute to this background. We measure this background using control samples in data. The probability for a non-prompt lepton to satisfy the isolation requirement ($I_{\text{rel}} < 0.15$) is measured in a data sample enriched with QCD dijet events, and varies from 2% to 3% for muons and from 6% to 8% for electrons as a function of lepton p_T .

Table 2: Relative systematic uncertainties for the mean WZ background. “On-Z” refers to events in which the OSSF pair satisfies $81 < M_{\ell\ell} < 101$ GeV. “Off-Z” refers to events with either $M_{\ell\ell} < 81$ GeV or $M_{\ell\ell} > 101$ GeV. The events are further categorized according to whether they have low (< 100 GeV) or high (> 100 GeV) M_T values. The “Off-Z, low- M_T ” column corresponds to the sum of events in regions I and V in Fig. 3, while the “Off-Z, high M_T ” column corresponds to the sum of regions II and IV.

	On-Z, high- M_T	Off-Z, low- M_T	Off-Z, high- M_T
Hadronic recoil	29.7%	0.9%	14.9%
WZ versus Z recoil	7.2%	0.5%	3.4 %
Lepton energy scale	1.8%	0.7%	0.7%
Lepton energy resolution	1.4%	6.9%	4.5%
Boson p_T	5.1%	0.4%	2.2%
Z mass shape	0.2%	0.4%	2.5%
Normalization	9.3%	9.3%	9.3%
Sum	32.4%	11.7%	18.8%

These probabilities, applied to the three-lepton events where the isolation requirement on one of the leptons is removed, are used to estimate background due to such non-prompt leptons.

Another background studied with data is the rare process in which a Z boson is accompanied by an initial- or final-state radiation photon that converts internally or externally, leading to a reconstructed three-lepton final state when the conversion is highly asymmetric [24].

The systematic uncertainties assigned to the $t\bar{t}$ background and other backgrounds studied with data are based on differences between the predicted and true yields when the method is applied to simulated events, as well as on the effect of the prompt-lepton contamination in control samples.

Backgrounds from very rare SM processes that have not yet been adequately measured in the data (ZZ, $t\bar{t}Z$, $t\bar{t}W$, three-vector-boson events) are estimated from simulation. For these sources, a systematic uncertainty of 50% is assigned to account for uncertainty in the NLO calculations of cross sections.

3.2.3 Observations in the three-lepton search with $M_{\ell\ell}$ and M_T

Figure 3 presents a scatter plot of M_T versus $M_{\ell\ell}$ for the selected events. The dashed lines divide the plane into six regions. The horizontal dashed line at $M_T = 100$ GeV separates the lower- M_T region, which contains most of the background associated with on-shell W bosons, from the region depleted of this background. The vertical dashed lines at $M_{\ell\ell} = 81$ GeV and 101 GeV define the endpoints of the region dominated by Z boson decays. In the lower $M_{\ell\ell}$ region, the search is sensitive to the signal production process of Fig. 1 with small to moderate $\tilde{\chi}_2^0 - \tilde{\chi}_1^0$ mass splittings (< 100 GeV), while being subject to background from $W + \gamma^*/Z^*$ events, especially in Region I. In the higher- $M_{\ell\ell}$ region, the search is sensitive to models with larger mass splittings. Region VI (on-Z, low M_T) is dominated by WZ and ZZ backgrounds. Leakage from this region contaminates the nearby regions.

Figure 4 shows the M_T distributions for data and the mean expected SM background below the Z (Regions I and II), on-Z (Regions III and VI), and above the Z (Regions IV and V). The background shape from non-prompt or misidentified leptons is taken from simulation while

the normalization is derived from the data.

Table 3 contains a summary of the mean estimated backgrounds and observed yields. There is no evidence for a signal, and the background shape is well reproduced within the limited statistics.

Table 3: Summary of mean expected backgrounds and observations in each region for the three-lepton search based on $M_{\ell\ell}$ and E_T^{miss} . Uncertainties include statistical and systematic contributions.

Region	WZ	Non-prompt	Rare SM	Total background	Data
I	16.2 ± 2.9	4.7 ± 2.4	2.1 ± 1.5	23.0 ± 5.1	31
II	3.6 ± 0.8	1.94 ± 1.02	0.4 ± 0.2	6.0 ± 1.3	3
III	15.6 ± 5.7	0.2 ± 0.1	0.8 ± 0.4	16.6 ± 5.7	17
IV	1.6 ± 0.4	0.2 ± 0.1	0.4 ± 0.2	2.2 ± 0.5	2
V	8.7 ± 1.7	1.4 ± 0.8	0.9 ± 0.4	11.0 ± 1.9	12
VI	150.6 ± 25.7	2.6 ± 1.4	11.7 ± 5.8	164.9 ± 26.4	173

Section 6 contains the detailed interpretation of these observations, which are found to have comparable sensitivity to the E_T^{miss} -based search of Section 3.1.

4 Searches in the same-sign two-lepton final state

Three-lepton final states are not sensitive to direct chargino-neutralino production if one of the leptons is unidentified, not isolated, or outside the acceptance of the analysis. The CMS

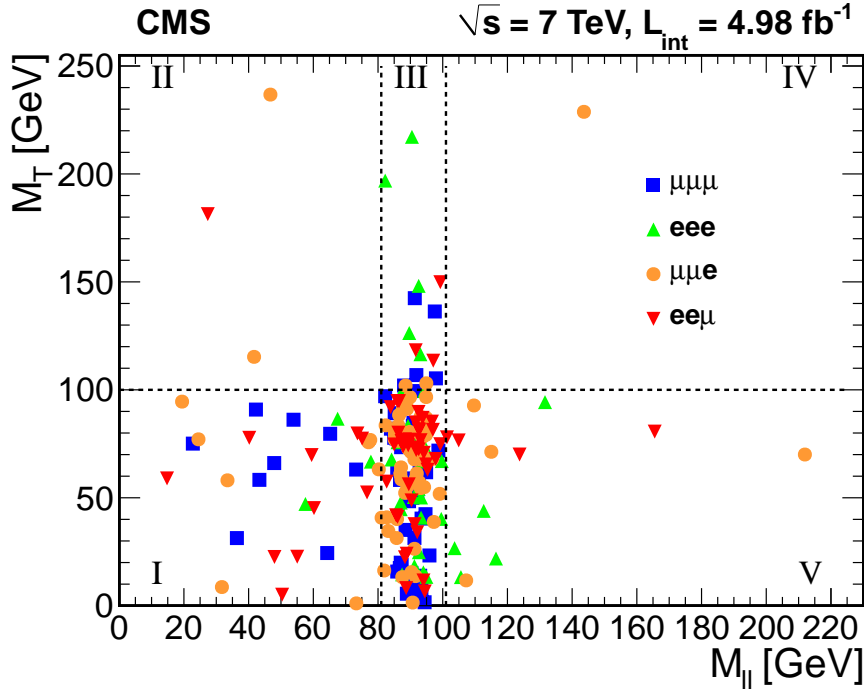


Figure 3: M_T versus $M_{\ell\ell}$ for the selected events in data. (Unlabeled Region VI lies between Regions I and V.) Two events appear outside the limits of the plot; one is a $\mu\mu\mu$ event at $(M_{\ell\ell}, M_T) = (240 \text{ GeV}, 399 \text{ GeV})$ and the other is an eee event at $(95 \text{ GeV}, 376 \text{ GeV})$.

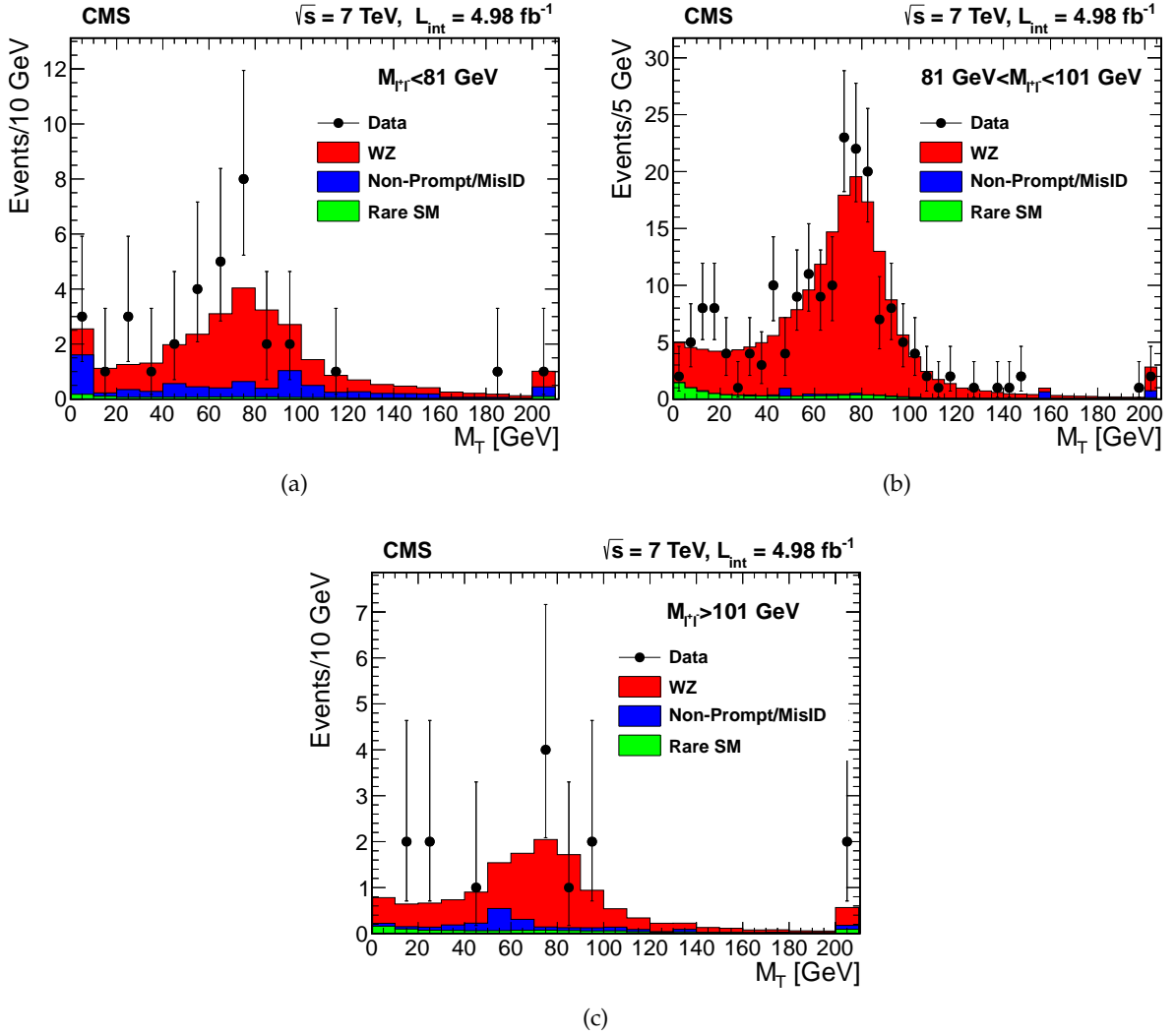


Figure 4: Observed and mean expected M_T distribution for $M_{\ell\ell}$ in the regions (a) below the Z boson mass, (b) on the Z boson mass, and (c) above the Z boson mass. Rare SM processes include three-vector-boson production, production of top-quark pairs together with a vector boson, and ZZ production. The last bin in each histogram includes the events with M_T beyond the histogram range.

detector has high geometrical acceptance for all leptons. However, when the signal-model mass splittings are such that one lepton has $p_T < 10$ GeV, three leptons are unlikely to be selected. Some of these otherwise-rejected events can be recovered by requiring only two leptons, which should however be of same sign (SS) to suppress the overwhelming background from opposite-sign dileptons [38, 66].

The SS dilepton search requires at least one electron or muon with $p_T > 20$ GeV, and another with $p_T > 10$ GeV, with $|\eta| < 2.4$ for both. We exclude events that contain a third lepton, using the criteria of Section 3.2, in order to facilitate combination with those results. Furthermore, as events with τ leptons can be important in some SUSY scenarios [67], we include the $e\tau$, $\mu\tau$, and $\tau\tau$ final states; for this purpose, we use hadronic decays of the τ . The isolation criteria for hadronically decaying τ leptons require that, apart from the hadronic decay products, there be

no charged hadron or photon with p_T above 0.8 GeV within a cone of $\Delta R = 0.5$ around the direction of the τ .

An important class of background for SS events is that with one genuine prompt lepton and either a non-prompt genuine lepton from a heavy-flavor decay or a misidentified hadron. This background arises mainly from events with jets and a W or Z boson. Much of the analysis strategy is driven by the need to suppress these events. Electron and muon selection criteria are thus tightened: the isolation criterion becomes $I_{\text{rel}} < 0.1$, and we add a criterion to limit the maximum energy deposit of muon candidates in the calorimeters.

Events containing OSSF pairs with $|M_{\ell\ell} - M_Z| < 15 \text{ GeV}$ are eliminated in order to reduce background due to processes such as WZ and $t\bar{t}Z$ production. For this purpose we select these events by using looser isolation criteria ($I_{\text{rel}} < 1.0$ for muons and barrel electrons, and $I_{\text{rel}} < 0.6$ for endcap electrons) and looser identification requirements for electrons.

The remaining background with a non-prompt lepton is estimated with techniques described in Ref. [26], where the probability for a non-prompt lepton to pass the signal selection is derived from control regions in data using extrapolations in the isolation and identification criteria. The systematic uncertainty on these predictions is 50% for light leptons and 30% for τ leptons.

Residual background is mostly due to charge misassignment in events with an OSSF pair, e.g., from Drell-Yan, $t\bar{t}$, or WW processes. We quantify the charge misassignment probability for electrons and τ leptons by studying SS ee or $\tau\tau$ events inside the Z mass peak region in data. For electrons, this probability is 0.0002 ± 0.0001 in the ECAL barrel and 0.0028 ± 0.0004 in the ECAL endcap, and for τ leptons it is 0.009 ± 0.024 . For muons, it is determined from cosmic-ray data to be of order 10^{-5} and is neglected.

Backgrounds of lesser importance include those from rare SM processes such as diboson production, associated production of a $t\bar{t}$ pair with a vector boson, or triboson production. They are taken from simulation with a 50% systematic uncertainty assigned. An exception is WZ production, for which normalization to the measured cross section is available, thus reducing the systematic uncertainty to 20%.

The distribution of events thus selected is studied in the plane of E_T^{miss} versus H_T , as displayed in Fig. 5(a). The signal region is defined by the criterion $E_T^{\text{miss}} > 200 \text{ GeV}$, with the $120 \text{ GeV} < E_T^{\text{miss}} < 200 \text{ GeV}$ interval used as a control region to confirm understanding of backgrounds. In the control region, the total mean expected background for events without a τ (ee , $\mu\mu$, and $e\mu$ events) is 24.8 ± 7.6 , and 27 events are observed. The total mean expected background for $e\tau$, $\mu\tau$, and $\tau\tau$ events is 24.5 ± 8.9 , and 26 events are observed. The observed signal region yields in the various lepton-flavor final states are displayed in Fig. 5(b). Table 4 presents the mean expected background and the observed yields in the signal region. Section 6 presents the detailed interpretation of these observations; combining the same-sign dilepton search with the three-lepton search increases the mass limits by up to approximately 20 GeV.

The same-sign analysis is potentially sensitive to the processes of Fig. 1 in the τ -dominated scenario, in which the chargino and neutralino both decay only to a τ . With the present selection, we are only able to exclude a limited region of phase space for this scenario, bounded by $m_{\tilde{\chi}_1^0} < 50 \text{ GeV}$ and $m_{\tilde{\chi}_2^0} = m_{\tilde{\chi}_1^\pm} < 250 \text{ GeV}$.

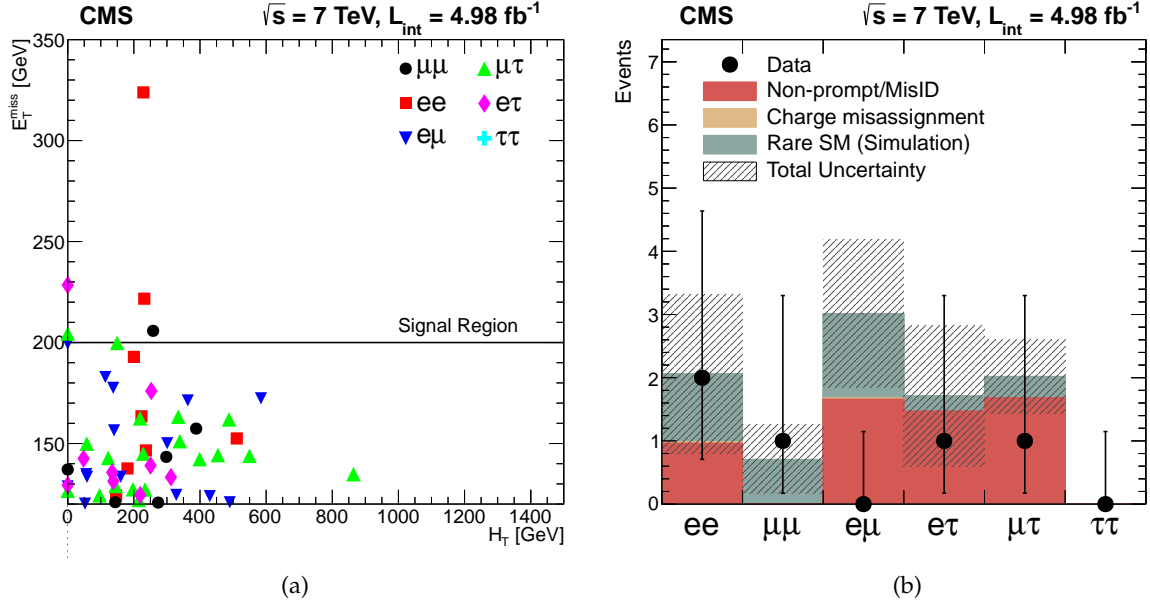


Figure 5: (a) E_T^{miss} versus H_T for same-sign dilepton candidate events. (b) Mean expected background yields with their uncertainty and observed number of events in the six channels, for the signal region ($E_T^{\text{miss}} > 200 \text{ GeV}$).

Table 4: Summary of mean expected backgrounds and observed yields in the $E_T^{\text{miss}} > 200 \text{ GeV}$ signal region for all six same-sign dilepton channels. The background categories comprise non-prompt and misidentified leptons, charge misassignment, and rare SM processes. Uncertainties include statistical and systematic contributions.

Source	ee	$\mu\mu$	$e\mu$	$e\tau$	$\mu\tau$	$\tau\tau$	Sum
Non-pr/misID	1.0 ± 0.8	0.0 ± 0.2	1.7 ± 1.0	1.5 ± 1.1	1.7 ± 0.6	0.00 ± 0.00	5.8 ± 1.9
Charge misass	0.0 ± 0.0	–	0.0 ± 0.0	0.0 ± 0.0	0.0 ± 0.1	0.00 ± 0.01	0.1 ± 0.1
Rare SM	1.0 ± 0.7	0.7 ± 0.5	1.3 ± 0.7	0.3 ± 0.1	0.4 ± 0.2	0.00 ± 0.00	3.7 ± 1.5
Total background	2.1 ± 1.0	0.7 ± 0.5	3.1 ± 1.2	1.7 ± 1.1	2.0 ± 0.6	0.00 ± 0.01	9.5 ± 2.4
Observed	2	1	0	1	1	0	5

5 Searches in the $WZ/ZZ + E_T^{\text{miss}}$ final state with two leptons and two jets

Finally, we consider events with two on-shell vector bosons and significant E_T^{miss} . Ref. [24] presents results relevant for the four-lepton final state, corresponding to the two-Z-boson process of Fig. 2(b), when each Z boson decays either to an electron or a muon pair. In the following, we extend sensitivity to both diagrams of Fig. 2 by selecting events in which a Z boson decays to either ee or $\mu\mu$, while a W boson or another Z boson decays to two jets. SM diboson events with the corresponding final states do not contain intrinsic E_T^{miss} .

This search is an extension of our previous result [25]. We use the same selection of jets, leptons, and E_T^{miss} , as well as the same background estimation methods. Both leptons must have $p_T > 20 \text{ GeV}$. In particular, jets are required to have $p_T > 30 \text{ GeV}$ and $|\eta| < 3$. The E_T^{miss} signal regions are indicated in Table 5, with the entries indicating mean background estimates after applying all selection criteria described below.

We suppress background from $t\bar{t}$ events by a factor of approximately 10 by rejecting events that contain an identified b jet. We use the TCHE loose (medium) working point for jets with $p_T < 100$ GeV (> 100 GeV). Further suppression of the $t\bar{t}$ and $Z + \text{jets}$ background is achieved by requiring that the dijet mass M_{jj} be consistent with a W or Z boson, namely $70 \text{ GeV} < M_{jj} < 110 \text{ GeV}$. Background from $WZ + \text{jets}$ events is suppressed by rejecting events that contain a third identified lepton with $p_T > 20$ GeV.

Background from SM $Z + \text{jets}$ events with artificial E_T^{miss} from jet mis-measurements must be carefully estimated, since the artificial E_T^{miss} is not necessarily well-reproduced in simulation. Using the method described in Ref [25], a control sample of $\gamma + \text{jets}$ events is used to model the E_T^{miss} in $Z + \text{jets}$ events, after performing a reweighting procedure to take into account the different kinematic properties of the hadronic systems in the control and signal samples.

Background processes with uncorrelated flavor, while dominated by $t\bar{t}$ events, also include events with $\tau\tau$ (via Drell-Yan production and followed by leptonic decays), WW , and single top production. For these processes, production in the same-flavor ee and $\mu\mu$ final states used for the search is modeled using a control sample of opposite-flavor (OF) $e\mu$ events. Subdominant background contributions from SM WZ and ZZ production are estimated from simulation.

The mean expected backgrounds in bins of E_T^{miss} and the observed yields are summarized in Table 5 and displayed in Fig. 6. Section 6 contains the interpretation of these results, including a combination with those of Ref. [24].

Table 5: Summary of mean expected backgrounds and observed data in each of the E_T^{miss} signal regions, in final states with two opposite-sign leptons, two jets, and E_T^{miss} . The total background is the sum of the $Z + \text{jets}$ background evaluated with $\gamma + \text{jets}$ events, the flavor-symmetric background evaluated from opposite-flavor events (OF background), and the WZ/ZZ background expected from simulation (WZ/ZZ background). Uncertainties include statistical and systematic contributions.

Source	$30 \leq E_T^{\text{miss}} < 60 \text{ GeV}$	$60 \leq E_T^{\text{miss}} < 80 \text{ GeV}$	$80 \leq E_T^{\text{miss}} < 100 \text{ GeV}$
Z + jets background	2298 ± 737	32.9 ± 11.1	5.2 ± 1.8
OF background	11 ± 2	6.6 ± 1.6	4.6 ± 1.2
WZ/ZZ background	50 ± 25	3.9 ± 2.0	2.2 ± 1.1
Total background	2359 ± 737	43.4 ± 11.4	12.0 ± 2.4
Data	2416	47	7

Source	$100 \leq E_T^{\text{miss}} < 150 \text{ GeV}$	$150 \leq E_T^{\text{miss}} < 200 \text{ GeV}$	$E_T^{\text{miss}} \geq 200 \text{ GeV}$
Z + jets background	1.7 ± 0.6	0.4 ± 0.2	0.20 ± 0.09
OF background	4.6 ± 1.2	0.8 ± 0.3	0.06 ± 0.07
WZ/ZZ background	2.5 ± 1.3	0.7 ± 0.4	0.4 ± 0.2
Total background	8.8 ± 1.8	1.9 ± 0.5	0.7 ± 0.3
Data	6	2	0

6 Interpretations of the searches

In this section, we present the interpretation of our results. Section 6.1 presents the limits on the SMS of Fig. 1 from the three-lepton search using the E_T^{miss} shape (Section 3.1). Section 6.2

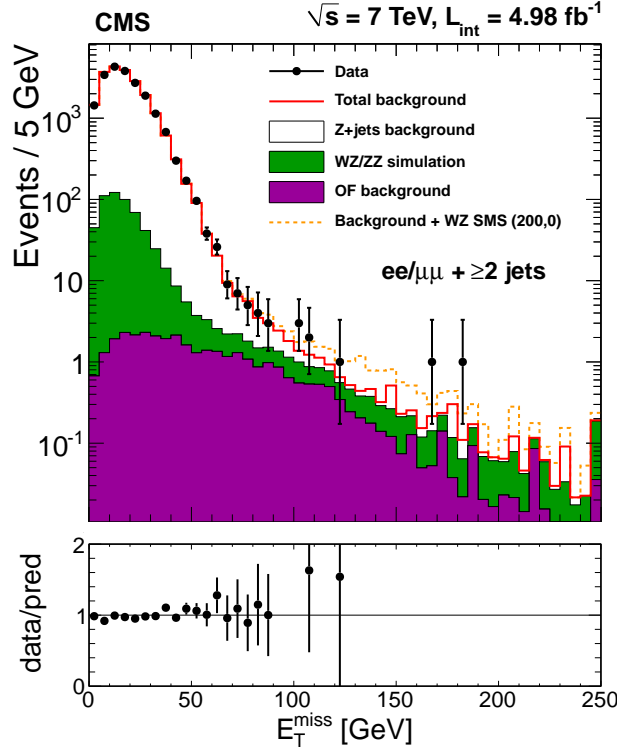


Figure 6: Observed E_T^{miss} distribution for $WZ + E_T^{\text{miss}}$ events after all selection criteria are applied except that on E_T^{miss} (solid points), in comparison with the corresponding SM expectation. For purposes of illustration, the E_T^{miss} distribution expected for WZ SMS events with $m_{\tilde{\chi}_2^0} = m_{\tilde{\chi}_1^\pm} = 200 \text{ GeV}$ and a massless LSP is shown. The plot below the main figure shows the ratio of the observed and mean-expected-background distributions.

presents the limits on the same SMS from the three-lepton search using $M_{\ell\ell}$ and M_T (Section 3.2), the same-sign dilepton search (Section 4), and their combination. Section 6.3 presents the limits on the SMS of Fig. 2 using results from Section 3 and from the $WZ + E_T^{\text{miss}}$ analysis of Section 5, as well as limits on a GMSB model using results from the $ZZ + E_T^{\text{miss}}$ analysis of Section 5 and the four-lepton results of Ref. [24]. In all the search channels, the observations agree with the expected background.

We present upper limits on the cross sections for pair production of charginos and neutralinos. All upper limits are computed at 95% confidence level (CL) using the CL_s criterion [68, 69] with choices in the implementation following those in Ref. [70]. Using the NLO cross section calculations from Ref. [50–52], we also evaluate 95% CL exclusion curves. The exclusion curves are shown not only for their central values, but also when the NLO cross section is varied by ± 1 standard deviation (σ) of its uncertainty [52]. In addition, we display the median expected exclusion limit in an ensemble of experiments with background only, as well as the uncertainty band that contains 68% of the limits in the ensembles.

6.1 Limits on SMS from the search with three leptons using E_T^{miss} shape

Figure 7(a) displays the 95% CL upper limits on the cross section times branching fraction in the $m_{\tilde{\chi}_1^0}$ versus $m_{\tilde{\chi}_2^0}$ ($= m_{\tilde{\chi}_1^\pm}$) plane, with $x_{\tilde{\chi}} = 0.5$ in the flavor-democratic scenario described in the Introduction. The contour bounds the excluded region in the plane assuming the NLO cross section calculation and a 50% branching fraction to three leptons, as appropriate for this SMS.

Figure 7(b) displays the corresponding limits for the τ -enriched scenario. The lower-sensitivity feature in the curve, noticeable where the common mass $m_{\tilde{\chi}_2^0} = m_{\tilde{\chi}_1^\pm}$ is approximately 100 GeV greater than $m_{\tilde{\chi}_1^0}$, corresponds to the phase space where the dilepton mass has a high probability to be close to the Z mass, such that the event is rejected.

6.2 Limits on SMS from the search with three leptons, $M_{\ell\ell}$, and M_T , and from same-sign dilepton searches

Figure 8 displays, for three values of $x_{\tilde{\ell}}$, the 95% CL upper limit on the chargino-neutralino production cross section times branching fraction in the flavor-democratic scenario, derived from the results of the three-lepton search using M_T and $M_{\ell\ell}$ and those of the SS dilepton search. The contours bound the mass regions excluded at 95% CL for a branching fraction of 50%, as appropriate for the visible decay products in this scenario. The contours based on the observations are shown for the separate searches and for the combination. This search has slightly better sensitivity than the complementary search based on the E_T^{miss} shape (Fig. 7) in the region where the difference between $m_{\tilde{\chi}_2^0} = m_{\tilde{\chi}_1^\pm}$ and $m_{\tilde{\chi}_1^0}$ is small, and slightly worse sensitivity where this mass difference is large.

Figure 9 presents the corresponding limits for the τ -enriched scenario. As the SS dilepton search does not have sensitivity for $x_{\tilde{\ell}} = 0.50$, there is no limit curve for this search in Fig. 9(b). In the other limit curves in both Figs. 8 and 9, the increase in the combined mass limit from

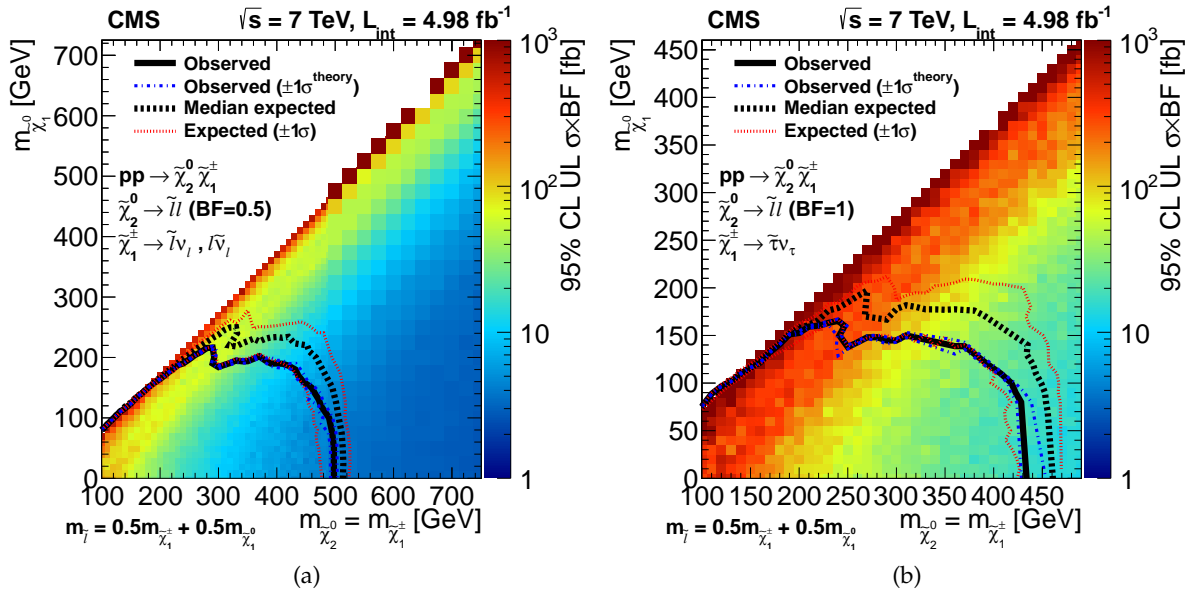


Figure 7: The shading in the $m_{\tilde{\chi}_1^0}$ versus $m_{\tilde{\chi}_2^0} (= m_{\tilde{\chi}_1^\pm})$ plane indicates the 95% CL upper limit on the chargino-neutralino NLO production cross section times branching fraction in (a) the flavor-democratic scenario, and (b) the τ -enriched scenario, based on the results of the three-lepton + E_T^{miss} search using the data of Ref. [24]. The slepton mass is the mean of the $\tilde{\chi}_1^0$ and $\tilde{\chi}_1^\pm$ masses, i.e., $x_{\tilde{\ell}} = 0.5$. In (a), the solid (dotted) contours bound the observed (expected) mass region excluded at 95% CL for a branching fraction of 50%, as appropriate for the three-lepton decay products in the flavor-democratic scenario. In (b), the same contours are for a branching fraction of 100%, as appropriate for the τ -enriched scenario, in which the final-state lepton from the chargino decay is always the τ lepton.

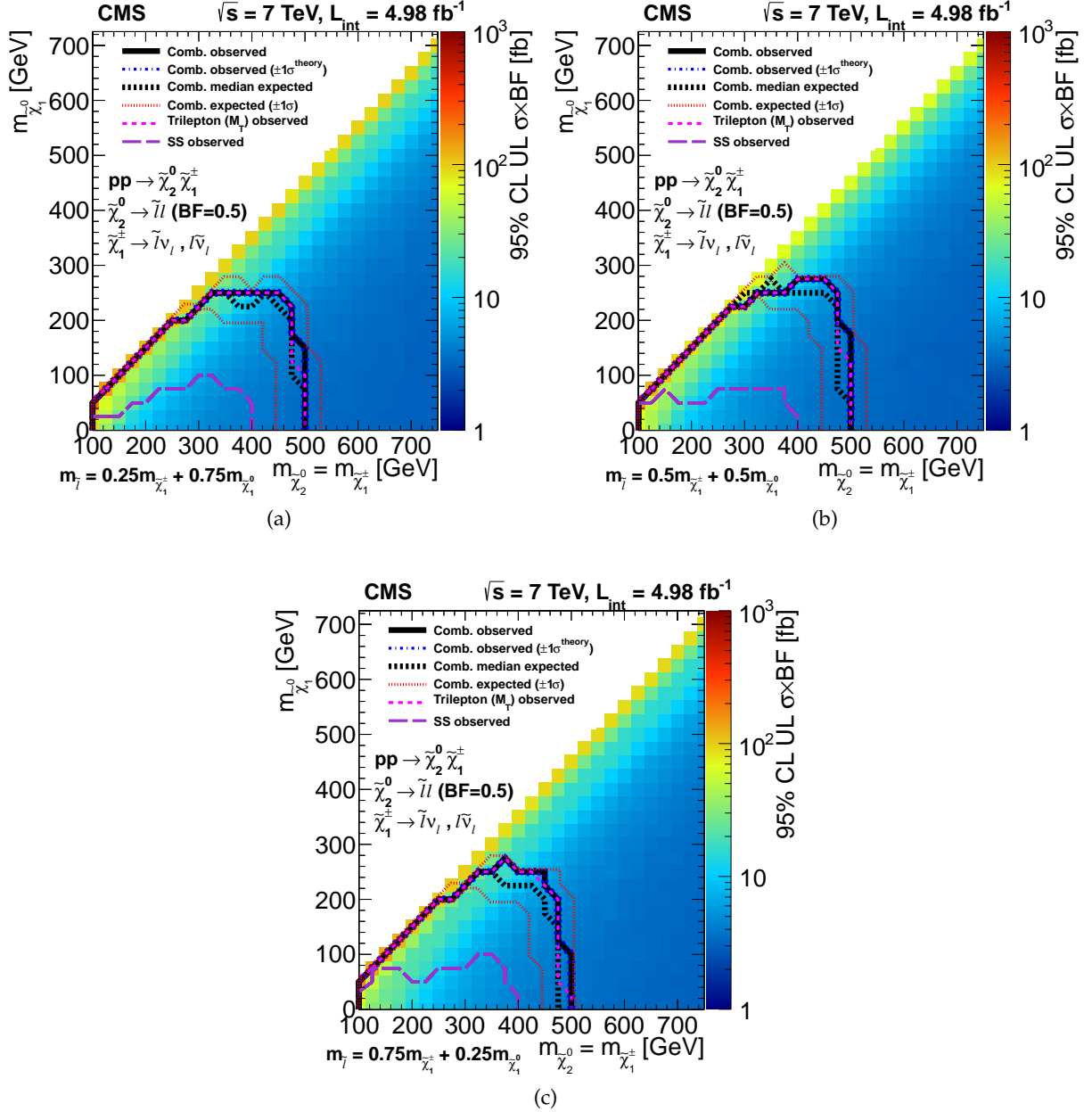


Figure 8: The shading in the $m_{\tilde{\chi}_1^0}$ versus $m_{\tilde{\chi}_2^0} (= m_{\tilde{\chi}_1^\pm})$ plane indicates the 95% CL upper limit on the chargino-neutralino production NLO cross section times branching fraction in the flavor-democratic scenario, for the combined analysis of the three-lepton search using $M_{\ell\ell}$ and M_T , and the same-sign dilepton search. The contours bound the mass regions excluded at 95% CL for a branching fraction of 50%, as appropriate for the visible decay products in this scenario. The contours based on the observations are shown for the separate searches and for the combination; in addition, the expected combined bound is shown. The three subfigures are the results for $x_{\tilde{\ell}}$ set to (a) 0.25, (b) 0.50, and (c) 0.75.

incorporation of the SS dilepton search ranges up to approximately 20 GeV.

Appendix A provides a prescription for emulating the event selection efficiency for this signature, in order to facilitate further interpretation of the results in electroweak SUSY production scenarios beyond the models considered in this paper.

6.3 Limits on SMS and GMSB from the WZ/ZZ + E_T^{miss} final state with two or more leptons

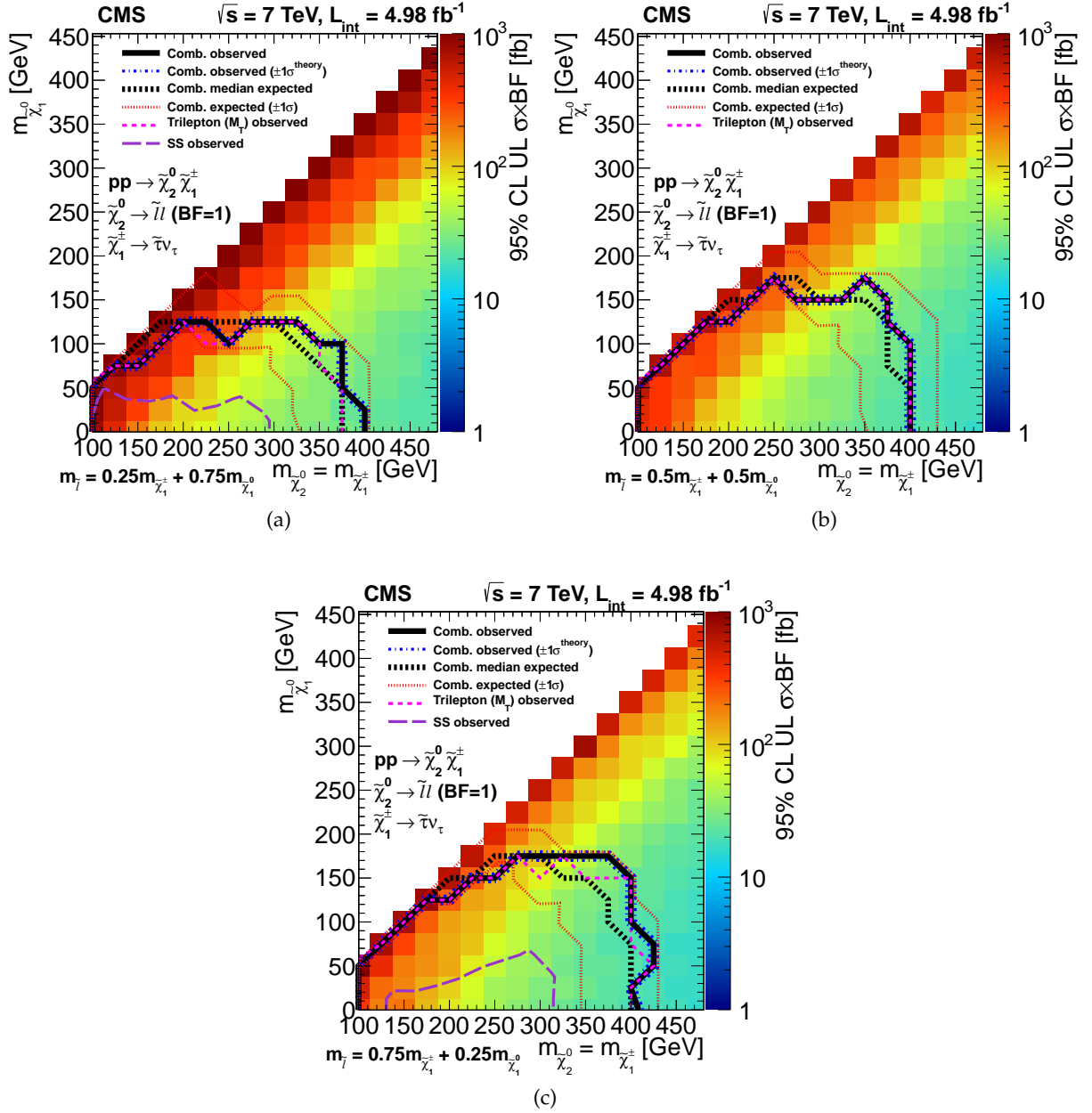
We calculate upper limits on the cross sections for pair production of charginos and neutralinos times branching fractions into the WZ + E_T^{miss} and ZZ + E_T^{miss} final states as a function of the chargino and neutralino masses. In calculating these limits, the uncertainties related to jet and E_T^{miss} quantities (jet multiplicity, dijet mass, and E_T^{miss}) vary significantly across the model space, and are addressed separately at each point, taking into account the bin-to-bin migration of signal events. The limits in Section 6.3.1 are presented in the context of the SMS of Fig. 2(a) with 100% branching fractions of the chargino (neutralino) to $W + \tilde{\chi}_1^\pm$ ($Z + \tilde{\chi}_1^0$). The wino-like cross section with coupling $g\gamma^\mu$ is assumed. As the present data do not have sufficient sensitivity to explore the SMS of Fig. 2(b), the limits in Section 6.3.2 are presented in the context of a gauge-mediated symmetry breaking (GMSB) Z-enriched higgsino model [35–37] that has a large branching fraction to the ZZ + E_T^{miss} final state. In this scenario, the LSP is a very light gravitino (mass ≤ 1 keV).

6.3.1 Limits on SMS with on-shell W and Z from WZ + E_T^{miss} and three-lepton analyses

For limits on the SMS of Fig. 2(a) with on-shell W and Z bosons, we combine the results of the WZ/ZZ + E_T^{miss} analysis and the three-lepton analysis of Section 3.2. From the WZ/ZZ + E_T^{miss} analysis, we use the results in exclusive E_T^{miss} regions, as summarized in Table 5. For the three-lepton analysis, we use the results in Table 3. The three-lepton region with the broadest sensitivity is Region III, the on-Z, high- M_T region. If the difference between the common mass $m_{\tilde{\chi}_2^0} = m_{\tilde{\chi}_1^\pm}$ and $m_{\tilde{\chi}_1^0}$ is small, then a significant fraction of the signal events fall below the Z mass window so that other signal regions contribute as well, in particular Region I (below-Z, low- M_T region). Region VI is not used directly in the fit, in order to facilitate the combination and to avoid using this region to constrain the WZ yield in the WZ/ZZ + E_T^{miss} analysis, where the kinematic selection is very different since it includes jet requirements. Instead, a scaling factor of 1.1 ± 0.1 is applied to the WZ yield in Regions I-V, based on the data/simulation comparison in Region VI.

In the combination, the common signal-related systematic uncertainties for luminosity, jet energy scale, lepton identification, trigger efficiency, and misidentification of light-flavor jets as b jets are considered to be 100% correlated. For backgrounds, the only common systematic uncertainty is that for the WZ/ZZ simulation, which is treated as 100% correlated. No events in the data pass both signal selections. For the backgrounds, the overlap in the control sample is less than 1%. Thus the two selections are treated as independent.

Figure 10 displays the observed limits for the two individual analyses and the combination. For large $m_{\tilde{\chi}_2^0} = m_{\tilde{\chi}_1^\pm}$, the WZ/ZZ + E_T^{miss} analysis has higher sensitivity due to the large hadronic branching fractions of the W and Z bosons. At lower $m_{\tilde{\chi}_2^0} = m_{\tilde{\chi}_1^\pm}$, the signal events do not have large E_T^{miss} , resulting in a loss of signal region acceptance for the WZ/ZZ + E_T^{miss} analysis. In this region, the background suppression provided by the requirement of a third lepton leads to better sensitivity for the three-lepton analysis.

Figure 9: For the τ -enriched scenario, the results corresponding to those in Fig. 8.

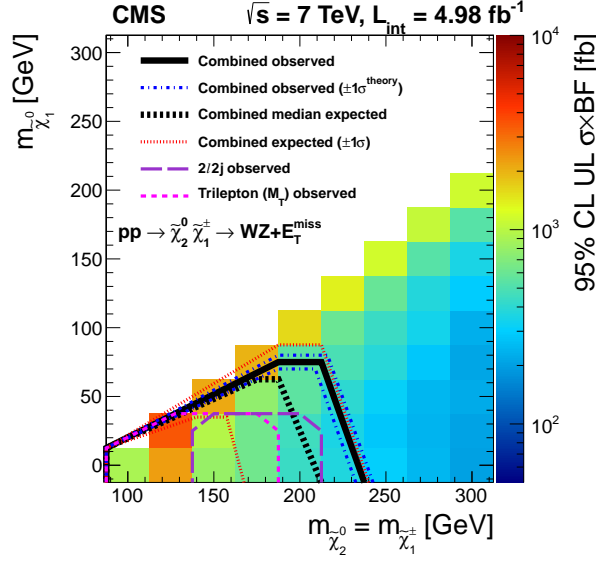


Figure 10: Interpretation of the $WZ + E_T^{\text{miss}}$ and three-lepton results in the context of the WZ SMS. The $WZ + E_T^{\text{miss}}$ observed, three-lepton observed, combined observed, and combined expected contours are indicated.

6.3.2 Limits on a Z-enriched GMSB model from $ZZ + E_T^{\text{miss}}$ and four-lepton search

For the SMS of Fig. 2(b) with two on-shell Z bosons, the present data do not exclude any region of $m_{\tilde{\chi}_2^0} = m_{\tilde{\chi}_1^\pm}$, and are therefore not sensitive to a scenario in which neutralino pair production is the sole production mechanism. However, the $ZZ + E_T^{\text{miss}}$ signature can be enhanced in scenarios in which additional mechanisms, such as chargino-chargino and chargino-neutralino production, also contribute. This is the case in a GMSB Z-enriched higgsino model [35–37].

In this scenario, the LSP is a nearly massless gravitino, the next-to-lightest SUSY particle is a Z-enriched higgsino $\tilde{\chi}_1^0$, and the $\tilde{\chi}_1^\pm$ is nearly mass degenerate with the $\tilde{\chi}_1^0$. We set the gaugino mass parameters M_1 and M_2 to $M_1 = M_2 = 1$ TeV, the ratio of Higgs expectation values $\tan\beta$ to $\tan\beta = 2$, and then explore variable Higgsino mass parameters. The masses of the $\tilde{\chi}_1^0$ and $\tilde{\chi}_1^\pm$ are controlled by the parameter μ , with $m_{\tilde{\chi}_1^0} \approx m_{\tilde{\chi}_1^\pm} \approx \mu$. Hence the $\tilde{\chi}_1^\pm$ decays to $\tilde{\chi}_1^0$ and to low- p_T SM particles that escape detection. Thus, all production mechanisms (chargino-chargino, chargino-neutralino, and neutralino-neutralino) lead to a pair of $\tilde{\chi}_1^0$ particles in the final state, and the branching fraction to the $ZZ + E_T^{\text{miss}}$ final state is large (varying from 100% at $\mu = 130$ GeV to 85% at $\mu = 410$ GeV). Mainly because of the mix of production mechanisms, the kinematic distributions of this model are slightly different than those expected in a pure neutralino-pair production scenario, leading to different signal acceptances.

We combine the results of the $WZ/ZZ + E_T^{\text{miss}}$ analysis of Section 5 with independent results for the four-lepton channel analysis of Ref. [24] to further restrict the GMSB scenario. The two selections have negligible overlap, and are thus treated as independent in the combination.

Table 6 summarizes the relevant results from Ref. [24], with the high- H_T and low- H_T regions of that study combined. All samples contain four leptons, including an OSSF lepton pair whose mass is consistent with the Z boson mass, with separate entries for events with E_T^{miss} above or below 50 GeV, and for events with zero or one hadronically decaying τ lepton candidate (τ_h).

The results of the individual and combined exclusions are displayed in Fig. 11. As in Sec-

Table 6: Summary of the results from the multilepton analysis of Ref. [24] used as input to the combined limit on the GMSB model. All categories have four leptons including an OSSF pair consistent with a Z boson; $N(\tau_h)$ denotes the number of these leptons that are identified as hadronically decaying τ leptons. Uncertainties include statistical and systematic contributions.

Signal Region	Expected Background	Observed Yield
$N(\tau_h) = 0, E_T^{\text{miss}} \geq 50 \text{ GeV}$	1.0 ± 0.2	1
$N(\tau_h) = 0, E_T^{\text{miss}} < 50 \text{ GeV}$	38 ± 15	34
$N(\tau_h) = 1, E_T^{\text{miss}} \geq 50 \text{ GeV}$	2.6 ± 0.7	4
$N(\tau_h) = 1, E_T^{\text{miss}} < 50 \text{ GeV}$	18.0 ± 5.2	20

tion 6.3.1, the $WZ/ZZ + E_T^{\text{miss}}$ and the multilepton analysis are complementary, with the four-lepton analysis having greater (less) sensitivity than the $WZ/ZZ + E_T^{\text{miss}}$ analysis at small (large) values of μ . By combining the two analyses, we exclude the range of μ between 148 and 248 GeV.

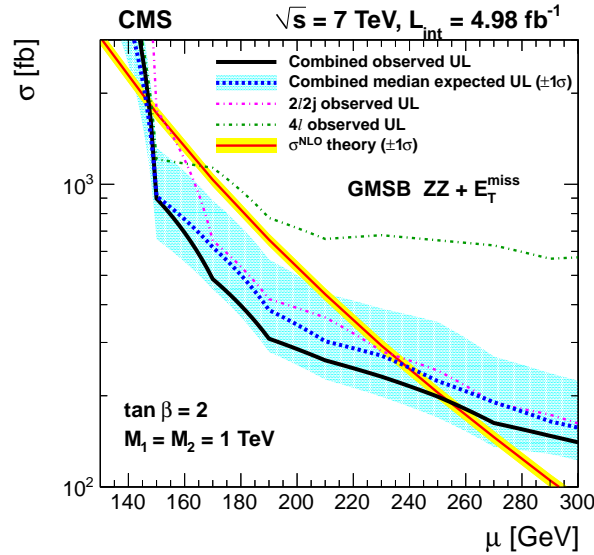


Figure 11: Interpretation of the results for the $ZZ + E_T^{\text{miss}}$ (with two leptons and two jets) analysis and the results of the four-lepton analysis from Ref. [24] in the context of the GMSB model described in the text. The NLO cross section upper limits are presented for the $ZZ + E_T^{\text{miss}}$ observed, multilepton observed, the combined observed, and the combined expected results. The theory prediction for the cross section is also presented. The median expected limits, their $\pm 1\sigma$ variations, and the $\pm 1\sigma$ band on the theory curve are as described at the beginning of Section 6.

6.4 Summary of excluded masses for chargino-neutralino pair production

Figure 12 displays a summary of the excluded regions in the chargino-neutralino production scenarios considered above. Also displayed are the exclusion curves at 95% CL from searches at LEP2 [16, 17, 71], which excluded $m_{\tilde{\ell}} < 82 \text{ GeV}$ and $m_{\tilde{\chi}_1^\pm} < 103 \text{ GeV}$. The results in this paper probe the production of charginos and neutralinos with masses up to approximately 200 to 500 GeV, depending on the decay modes of these particles.

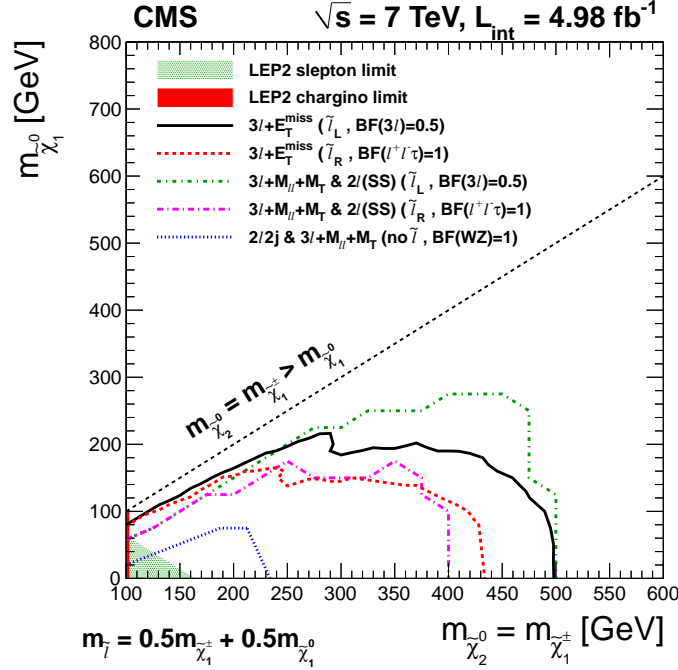


Figure 12: Summary of the excluded regions in the $m_{\tilde{\chi}_1^0}$ versus $m_{\tilde{\chi}_2^0}$ ($= m_{\tilde{\chi}_1^\pm}$) plane for: the three-lepton+ E_T^{miss} search (Sections 3.1 and 6.1), separately for the $\tilde{\ell}_L$ and $\tilde{\ell}_R$ scenarios; the combination (Section 6.2) of the three-lepton analysis based on $M_{\ell\ell}$ and M_T (Section 3.2) with the SS dilepton analysis (Section 4), separately for the $\tilde{\ell}_L$ and $\tilde{\ell}_R$ scenarios; and the combination (Section 6.3.1) of the diboson analysis with two leptons and two jets (Section 5) with the three-lepton analysis based on $M_{\ell\ell}$ and M_T (Section 3.2), for the $WZ + E_T^{\text{miss}}$ model. Regions excluded by searches at LEP2 for sleptons and charginos are also indicated. The implied branching fractions introduced in Section 1 are noted in the legend. For models with intermediate sleptons (including the LEP2 slepton limit), the interpretations correspond to $x_{\tilde{\ell}} = 0.5$.

7 Summary

This paper presents searches for supersymmetric charginos and neutralinos. While a number of previous studies at the LHC have focused on strongly coupled supersymmetric particles, this paper is one of the first to focus on the electroweak sector of supersymmetry. The searches performed here explore final states with exactly three leptons using transverse mass and lepton-pair invariant mass, two same-sign leptons, and two opposite-sign leptons and two jets. The results of a published search for new physics in the final state of three or more leptons are reinterpreted in the context of electroweak supersymmetry. No excesses above the standard model expectations are observed. The results are used to exclude a range of chargino and neutralino masses from approximately 200 to 500 GeV in the context of models that assume large branching fractions of charginos and neutralinos to leptons and vector bosons.

Acknowledgements

We thank David Shih for useful discussions and help with implementation of the Z-enriched GMSB model of Section 6.3.2.

We congratulate our colleagues in the CERN accelerator departments for the excellent performance of the LHC machine. We thank the technical and administrative staff at CERN and other CMS institutes. This work was supported by the Austrian Federal Ministry of Science and Research; the Belgian Fonds de la Recherche Scientifique, and Fonds voor Wetenschappelijk Onderzoek; the Brazilian Funding Agencies (CNPq, CAPES, FAPERJ, and FAPESP); the Bulgarian Ministry of Education and Science; CERN; the Chinese Academy of Sciences, Ministry of Science and Technology, and National Natural Science Foundation of China; the Colombian Funding Agency (COLCIENCIAS); the Croatian Ministry of Science, Education and Sport; the Research Promotion Foundation, Cyprus; the Ministry of Education and Research, Recurrent financing contract SF0690030s09 and European Regional Development Fund, Estonia; the Academy of Finland, Finnish Ministry of Education and Culture, and Helsinki Institute of Physics; the Institut National de Physique Nucléaire et de Physique des Particules / CNRS, and Commissariat à l'Énergie Atomique et aux Énergies Alternatives / CEA, France; the Bundesministerium für Bildung und Forschung, Deutsche Forschungsgemeinschaft, and Helmholtz-Gemeinschaft Deutscher Forschungszentren, Germany; the General Secretariat for Research and Technology, Greece; the National Scientific Research Foundation, and National Office for Research and Technology, Hungary; the Department of Atomic Energy and the Department of Science and Technology, India; the Institute for Studies in Theoretical Physics and Mathematics, Iran; the Science Foundation, Ireland; the Istituto Nazionale di Fisica Nucleare, Italy; the Korean Ministry of Education, Science and Technology and the World Class University program of NRF, Korea; the Lithuanian Academy of Sciences; the Mexican Funding Agencies (CINVESTAV, CONACYT, SEP, and UASLP-FAI); the Ministry of Science and Innovation, New Zealand; the Pakistan Atomic Energy Commission; the Ministry of Science and Higher Education and the National Science Centre, Poland; the Fundação para a Ciência e a Tecnologia, Portugal; JINR (Armenia, Belarus, Georgia, Ukraine, Uzbekistan); the Ministry of Education and Science of the Russian Federation, the Federal Agency of Atomic Energy of the Russian Federation, Russian Academy of Sciences, and the Russian Foundation for Basic Research; the Ministry of Science and Technological Development of Serbia; the Secretaría de Estado de Investigación, Desarrollo e Innovación and Programa Consolider-Ingenio 2010, Spain; the Swiss Funding Agencies (ETH Board, ETH Zurich, PSI, SNF, UniZH, Canton Zurich, and SER); the National Science Council, Taipei; the Thailand Center of Excellence in Physics, the Institute for the Promotion of Teaching Science and Technology and National Electronics and Computer Technology Center; the Scientific and Technical Research Council of Turkey, and Turkish Atomic Energy Authority; the Science and Technology Facilities Council, UK; the US Department of Energy, and the US National Science Foundation.

Individuals have received support from the Marie-Curie programme and the European Research Council (European Union); the Leventis Foundation; the A. P. Sloan Foundation; the Alexander von Humboldt Foundation; the Austrian Science Fund (FWF); the Belgian Federal Science Policy Office; the Fonds pour la Formation à la Recherche dans l'Industrie et dans l'Agriculture (FRIA-Belgium); the Agentschap voor Innovatie door Wetenschap en Technologie (IWT-Belgium); the Ministry of Education, Youth and Sports (MEYS) of Czech Republic; the Council of Science and Industrial Research, India; the Compagnia di San Paolo (Torino); and the HOMING PLUS programme of Foundation for Polish Science, cofinanced from European Union, Regional Development Fund.

References

- [1] Y. A. Golfand and E. P. Likhtman, "Extension of the algebra of Poincare group generators and violation of P invariance", *JETP Lett.* **13** (1971) 323.
- [2] P. Ramond, "Dual theory for free fermions", *Phys. Rev. D* **3** (1971) 2415, doi:10.1103/PhysRevD.3.2415.
- [3] A. Neveu and J. H. Schwarz, "Factorizable dual model of pions", *Nucl. Phys. B* **31** (1971) 86, doi:10.1016/0550-3213(71)90448-2.
- [4] A. Neveu and J. H. Schwarz, "Quark model of dual pions", *Phys. Rev. D* **4** (1971) 1109, doi:10.1103/PhysRevD.4.1109.
- [5] D. V. Volkov and V. P. Akulov, "Is the neutrino a goldstone particle?", *Phys. Lett. B* **46** (1973) 109, doi:10.1016/0370-2693(73)90490-5.
- [6] J. Wess and B. Zumino, "A lagrangian model invariant under supergauge transformations", *Phys. Lett. B* **49** (1974) 52, doi:10.1016/0370-2693(74)90578-4.
- [7] J. Wess and B. Zumino, "Supergauge transformations in four-dimensions", *Nucl. Phys. B* **70** (1974) 39, doi:10.1016/0550-3213(74)90355-1.
- [8] D. A. Dicus, S. Nandi, and X. Tata, "W decay in supergravity GUTS", *Phys. Lett. B* **129** (1983) 451, doi:10.1016/0370-2693(83)90138-7.
- [9] A. H. Chamseddine, P. Nath, and R. L. Arnowitt, "Experimental signals for supersymmetric decays of the W and Z bosons", *Phys. Lett. B* **129** (1983) 445, doi:10.1016/0370-2693(83)90137-5.
- [10] H. Baer and X. Tata, "Multi-lepton signals from W^\pm and Z^0 decays to gauginos at $\bar{p}p$ colliders", *Phys. Lett. B* **155** (1985) 278, doi:10.1016/0370-2693(85)90654-9.
- [11] P. Nath and R. L. Arnowitt, "Supersymmetric signals at the Tevatron", *Mod. Phys. Lett. A* **2** (1987) 331, doi:10.1142/S0217732387000446.
- [12] H. Baer, C.-h. Chen, F. Paige et al., "Trileptons from chargino - neutralino production at the CERN Large Hadron Collider", *Phys. Rev. D* **50** (1994) 4508, doi:10.1103/PhysRevD.50.4508.
- [13] H. Baer, C.-h. Chen, F. Paige et al., "Signals for minimal supergravity at the CERN Large Hadron Collider. II: multilepton channels", *Phys. Rev. D* **53** (1996) 6241, doi:10.1103/PhysRevD.53.6241.
- [14] CMS Collaboration, "Absolute calibration of the luminosity measurement at CMS: winter 2012 update", CMS Physics Analysis Summary CMS-PAS-SMP-12-008, (2012).
- [15] ALEPH Collaboration, "Absolute mass lower limit for the lightest neutralino of the MSSM from e^+e^- data at \sqrt{s} up to 209 GeV", *Phys. Lett. B* **583** (2004) 247, doi:10.1016/j.physletb.2003.12.066. See also references therein.
- [16] ALEPH Collaboration, "Absolute lower limits on the masses of selectrons and sneutrinos in the MSSM", *Phys. Lett. B* **544** (2002) 73, doi:10.1016/S0370-2693(02)02471-1.

- [17] DELPHI Collaboration, “Searches for supersymmetric particles in e^+e^- collisions up to 208 GeV and interpretation of the results within the MSSM”, *Eur. Phys. J. C* **31** (2003) 421, doi:10.1140/epjc/s2003-01355-5. See also references therein.
- [18] L3 Collaboration, “Search for scalar leptons and scalar quarks at LEP”, *Phys. Lett. B* **580** (2004) 37, doi:10.1016/j.physletb.2003.10.010. See also references therein.
- [19] OPAL Collaboration, “Search for chargino and neutralino production at $\sqrt{s} = 192 - 209$ GeV at LEP”, *Eur. Phys. J. C* **35** (2004) 1, doi:10.1140/epjc/s2004-01758-8. See also references therein.
- [20] CDF Collaboration, “Search for supersymmetry in $p\bar{p}$ collisions at $\sqrt{s} = 1.96$ -TeV using the trilepton signature for chargino-neutralino production”, *Phys. Rev. Lett.* **101** (2008) 251801, doi:10.1103/PhysRevLett.101.251801.
- [21] D0 Collaboration, “Search for associated production of charginos and neutralinos in the trilepton final state using 2.3 fb^{-1} of data”, *Phys. Lett. B* **680** (2009) 34, doi:10.1016/j.physletb.2009.08.011.
- [22] ATLAS Collaboration, “Search for supersymmetry in events with three leptons and missing transverse momentum in $\sqrt{s} = 7$ TeV pp collisions with the ATLAS detector”, *Phys. Rev. Lett.* **108** (2012) 261804, doi:10.1103/PhysRevLett.108.261804.
- [23] CMS Collaboration, “Search for physics beyond the standard model using multilepton signatures in pp collisions at $\sqrt{s} = 7$ TeV”, *Phys. Lett. B* **704** (2011) 411, doi:10.1016/j.physletb.2011.09.047.
- [24] CMS Collaboration, “Search for anomalous production of multilepton events in pp collisions at $\sqrt{s} = 7$ TeV”, *JHEP* **06** (2012) 169, doi:10.1007/JHEP06(2012)169.
- [25] CMS Collaboration, “Search for physics beyond the standard model in events with a Z boson, jets, and missing transverse energy in pp collisions at $\sqrt{s} = 7$ TeV”, (2012). arXiv:1204.3774. Accepted by *Phys. Lett. B*.
- [26] CMS Collaboration, “Search for new physics with same-sign isolated dilepton events with jets and missing transverse energy”, (2012). arXiv:1205.6615. Submitted to *Phys. Rev. Lett.*
- [27] B. Knuteson and S. Mrenna, “BARD: interpreting new frontier energy collider physics”, (2006). arXiv:hep-ph/0602101.
- [28] N. Arkani-Hamed, P. Schuster, N. Toro et al., “MARMOSSET: the path from LHC data to the new standard model via on-shell effective theories”, (2007). arXiv:hep-ph/0703088.
- [29] S. Dube, J. Glatzer, S. Somalwar et al., “Addressing the multi-channel inverse problem at high energy colliders: a model-independent approach to the search for new physics with trileptons”, *J. Phys. G* **39** (2012) 085004, doi:10.1088/0954-3899/39/8/085004.
- [30] J. Alwall, P. Schuster, and N. Toro, “Simplified models for a first characterization of new physics at the LHC”, *Phys. Rev. D* **79** (2009) 075020, doi:10.1103/PhysRevD.79.075020.
- [31] J. Alwall, M.-P. Le, M. Lisanti et al., “Model-independent jets plus missing energy searches”, *Phys. Rev. D* **79** (2009) 015005, doi:10.1103/PhysRevD.79.015005.

- [32] D. Alves et al., “Simplified models for LHC new physics searches”, (2011).
arXiv:1105.2838.
- [33] D. S. M. Alves, E. Izaguirre, and J. G. Wacker, “Where the sidewalk ends: jets and missing energy search strategies for the 7 TeV LHC”, *JHEP* **10** (2011) 012,
doi:10.1007/JHEP10(2011)012.
- [34] M. Papucci, J. Ruderman, and A. Weiler, “Natural SUSY endures”, (2011).
arXiv:1110.6926.
- [35] K. T. Matchev and S. D. Thomas, “Higgs and Z boson signatures of supersymmetry”,
Phys. Rev. D **62** (2000) 077702, doi:10.1103/PhysRevD.62.077702.
- [36] P. Meade, M. Reece, and D. Shih, “Prompt decays of general neutralino NLSPs at the Tevatron”, *JHEP* **05** (2010) 105, doi:10.1007/JHEP05(2010)105.
- [37] J. T. Ruderman and D. Shih, “General neutralino NLSPs at the early LHC”, (2011).
arXiv:1103.6083.
- [38] K. T. Matchev and D. M. Pierce, “Supersymmetry reach of the Tevatron via trilepton, like sign dilepton and dilepton plus τ jet signatures”, *Phys. Rev. D* **60** (1999) 075004,
doi:10.1103/PhysRevD.60.075004.
- [39] H. Baer, M. Drees, F. Paige et al., “Trilepton signal for supersymmetry at the Fermilab Tevatron revisited”, *Phys. Rev. D* **61** (2000) 095007,
doi:10.1103/PhysRevD.61.095007.
- [40] K. T. Matchev and D. M. Pierce, “New backgrounds in trilepton, dilepton and dilepton plus τ jet SUSY signals at the Tevatron”, *Phys. Lett. B* **467** (1999) 225,
doi:10.1016/S0370-2693(99)01155-7.
- [41] V. D. Barger and C. Kao, “Trilepton signature of minimal supergravity at the upgraded Tevatron”, *Phys. Rev. D* **60** (1999) 115015, doi:10.1103/PhysRevD.60.115015.
- [42] ATLAS Collaboration, “Search for direct production of charginos and neutralinos in events with three leptons and missing transverse momentum in $\sqrt{s} = 7$ TeV pp collisions with the ATLAS detector”, (2012). arXiv:1208.3144. Submitted to *Phys. Lett. B*.
- [43] ATLAS Collaboration, “Search for direct slepton and gaugino production in final states with two leptons and missing transverse momentum with the ATLAS detector in pp collisions at $\sqrt{s} = 7$ TeV”, (2012). arXiv:1208.2884. Submitted to *Phys. Lett. B*.
- [44] CMS Collaboration, “The CMS experiment at the CERN LHC”, *JINST* **3** (2008) S08004,
doi:10.1088/1748-0221/3/08/S08004.
- [45] F. Maltoni and T. Stelzer, “MadEvent: automatic event generation with MadGraph”,
JHEP **02** (2003) 027, doi:10.1088/1126-6708/2003/02/027.
- [46] J. Alwall, M. Herquet, F. Maltoni et al., “MadGraph 5: going beyond”, *JHEP* **06** (2011) 128,
doi:10.1007/JHEP06(2011)128.
- [47] T. Sjöstrand, S. Mrenna, and P. Z. Skands, “A brief introduction to PYTHIA 8.1”, *Comput. Phys. Commun.* **178** (2008) 852, doi:10.1016/j.cpc.2008.01.036.

- [48] P. M. Nadolsky, H.-L. Lai, Q.-H. Cao et al., “Implications of CTEQ global analysis for collider observables”, *Phys. Rev. D* **78** (2008) 013004, doi:10.1103/PhysRevD.78.013004.
- [49] J. M. Campbell, R. Ellis, and C. Williams, “Vector boson pair production at the LHC”, *JHEP* **07** (2011) 018, doi:10.1007/JHEP07(2011)018.
- [50] W. Beenakker, M. Klasen, M. Krämer et al., “Production of charginos, neutralinos, and sleptons at hadron colliders”, *Phys. Rev. Lett.* **83** (1999) 3780, doi:10.1103/PhysRevLett.83.3780.
- [51] W. Beenakker, M. Klasen, M. Krämer et al., “Erratum: production of charginos, neutralinos, and sleptons at hadron colliders”, *Phys. Rev. Lett.* **100** (2008) 029901, doi:10.1103/PhysRevLett.100.029901.
- [52] M. Krämer, A. Kulesza, R. van der Leeuw et al., “Supersymmetry production cross sections in pp collisions at $\sqrt{s} = 7$ TeV”, (2012). arXiv:1206.2892.
- [53] P. Z. Skands et al., “SUSY Les Houches accord: interfacing SUSY spectrum calculators, decay packages, and event generators”, *JHEP* **07** (2004) 036, doi:10.1088/1126-6708/2004/07/036.
- [54] H. Baer, F. E. Paige, S. D. Protopopescu et al., “Simulating supersymmetry with ISAJET 7.0 / ISASUSY 1.0”, (1993). arXiv:hep-ph/9305342.
- [55] W. Beenakker, R. Hoepker, and M. Spira, “PROSPINO: a program for the production of supersymmetric particles in next-to-leading order QCD”, (1996). arXiv:hep-ph/9611232.
- [56] CMS Collaboration, “The fast simulation of the CMS Detector at the LHC”, in *International Conference on Computing in High Energy and Nuclear Physics (CHEP 2010)*. *J. Phys.: Conference Series* **331** (2011) 032049. doi:10.1088/1742-6596/331/3/032049.
- [57] S. Agostinelli et al., “GEANT4 – a simulation toolkit”, *Nucl. Instr. Meth. A* **506** (2003) 250, doi:10.1016/S0168-9002(03)01368-8.
- [58] CMS Collaboration, “Study of tau reconstruction algorithms using pp collisions data collected at $\sqrt{s} = 7$ TeV”, CMS Physics Analysis Summary CMS-PAS-PFT-10-004, (2010).
- [59] CMS Collaboration, “CMS strategies for tau reconstruction and identification using particle-flow techniques”, CMS Physics Analysis Summary CMS-PAS-PFT-08-001, (2009).
- [60] CMS Collaboration, “Electron reconstruction and identification at $\sqrt{s} = 7$ TeV”, CMS Physics Analysis Summary CMS-PAS-EGM-10-004, (2010).
- [61] CMS Collaboration, “Performance of CMS muon reconstruction in pp collision events at $\sqrt{s} = 7$ TeV”, (2012). arXiv:1206.4071. Submitted to *JINST*.
- [62] CMS Collaboration, “Performance of τ lepton reconstruction and identification in CMS”, *JINST* **7** (2012) P01001, doi:10.1088/1748-0221/7/01/P01001.
- [63] M. Cacciari, G. P. Salam, and G. Soyez, “The anti- k_t jet clustering algorithm”, *JHEP* **04** (2008) 063, doi:10.1088/1126-6708/2008/04/063.
- [64] CMS Collaboration, “Performance of the b-jet identification in CMS”, CMS Physics Analysis Summary CMS-PAS-BTV-11-001, (2011).

- [65] CMS Collaboration, “Measurement of the inclusive W and Z production cross sections in pp collisions at $\sqrt{s} = 7$ TeV with the CMS experiment”, *JHEP* **10** (2011) 132, doi:10.1007/JHEP10(2011)132.
- [66] J. Nachtman, D. Saltzberg, and M. Worcester, “Study of a like sign dilepton search for chargino neutralino production at CDF”, (1999). arXiv:hep-ex/9902010. FERMILAB-CONF-99-023-E.
- [67] J. D. Lykken and K. T. Matchev, “Supersymmetry signatures with τ jets at the Tevatron”, *Phys. Rev. D* **61** (2000) 015001, doi:10.1103/PhysRevD.61.015001.
- [68] T. Junk, “Confidence level computation for combining searches with small statistics”, *Nucl. Instrum. Meth. A* **434** (1999) 435, doi:10.1016/S0168-9002(99)00498-2.
- [69] A. L. Read, “Presentation of search results: The CL_s technique”, *J. Phys. G* **28** (2002) 2693, doi:10.1088/0954-3899/28/10/313.
- [70] ATLAS and CMS Collaborations, “Procedure for the LHC Higgs boson search combination in summer 2011”, Technical Report ATL-PHYS-PUB-2011-11, CMS-NOTE-2011-005, Geneva, (2011).
- [71] Particle Data Group, J. Beringer, et al., “Review of particle physics”, *Phys. Rev. D* **86** (2012) 010001, doi:10.1103/PhysRevD.86.010001.

A Signal efficiency model for the three-lepton analysis with $M_{\ell\ell}$ and M_T

In order to facilitate the interpretation of the three-lepton results with $M_{\ell\ell}$ and M_T presented in Section 3.2 within the context of other signal models that are not considered here, we provide a prescription for emulating the event selection efficiency. This prescription includes lepton reconstruction and identification efficiencies, E_T^{miss} and M_T selection efficiencies, as well as the b-jet identification probability. The latter can be used to parameterize the b-veto acceptance in case the model of interest contains such jets.

We perform a fit to efficiency curves for each selection using the parametric function

$$\epsilon(x) = p_6 + p_4 \left[\text{erf} \left(\frac{x - p_0}{p_1} \right) + 1 \right] + p_5 \left[\text{erf} \left(\frac{x - p_2}{p_3} \right) + 1 \right], \quad (5)$$

where x represents the observable for which the efficiency is parametrized, and erf indicates the error function. This includes the efficiency for electrons and muons to be reconstructed and to satisfy the identification requirements as a function of the lepton p_T ; the probability for an event to satisfy the requirements $E_T^{\text{miss}} > 50 \text{ GeV}$ and $M_T > 100 \text{ GeV}$ as a function of true E_T^{miss} and true M_T ; and the probability for a jet to be identified as a b jet separately for the cases where the jet originates from a b-, c-, or light-flavor quark or gluon as a function of jet p_T . (The true E_T^{miss} observable is calculated with the stable generator-level invisible particles, while the true M_T is calculated using the true E_T^{miss} and the third lepton, i.e., the one not used in the $M_{\ell\ell}$ calculation.)

The parameters of the fitted functions are given in Table 7. Using these parameters and the values of x , a combined probability for a given event to pass the full event selection can be obtained. We have tested the efficiency model in a signal sample and observed consistent event yields compared to the full detector simulation within about 25%.

Table 7: The parameters of the efficiency function $\epsilon(x)$, where x represents $p_T(\mu)$, $p_T(e)$, E_T^{miss} , M_T , or $p_T(\text{parton})$ for different quark flavors (udscb) and for gluons (g).

x	p_0	p_1	p_2	p_3	p_4	p_5	p_6
$p_T(\mu)$	-4.65	27.38	-14.64	-9.31	0.47	-849.3	0.
$p_T(e)$,	12.32	10.11	20.12	32.17	0.32	0.11	0.
E_T^{miss}	48.37	43.54	49.90	14.95	0.06	0.44	0.
M_T	98.23	87.99	97.61	29.78	0.36	0.14	0.008
$p_T(\text{b quark})$	30.60	31.80	0.34	0.	0.	0.	0.
$p_T(\text{c quark})$	32.02	45.34	0.11	0.	0.	0.	0.
$p_T(\text{udsg parton})$	68.84	55.21	0.02	0.	0.	0.	0.

B The CMS Collaboration

Yerevan Physics Institute, Yerevan, Armenia

S. Chatrchyan, V. Khachatryan, A.M. Sirunyan, A. Tumasyan

Institut für Hochenergiephysik der OeAW, Wien, Austria

W. Adam, E. Aguilo, T. Bergauer, M. Dragicevic, J. Erö, C. Fabjan¹, M. Friedl, R. Frühwirth¹, V.M. Ghete, J. Hammer, N. Hörmann, J. Hrubec, M. Jeitler¹, W. Kiesenhofer, V. Knünz, M. Krammer¹, I. Krätschmer, D. Liko, I. Mikulec, M. Pernicka[†], B. Rahbaran, C. Rohringer, H. Rohringer, R. Schöfbeck, J. Strauss, A. Taurok, W. Waltenberger, G. Walzel, E. Widl, C.-E. Wulz¹

National Centre for Particle and High Energy Physics, Minsk, Belarus

V. Mossolov, N. Shumeiko, J. Suarez Gonzalez

Universiteit Antwerpen, Antwerpen, Belgium

M. Bansal, S. Bansal, T. Cornelis, E.A. De Wolf, X. Janssen, S. Luyckx, L. Mucibello, S. Ochesanu, B. Roland, R. Rougny, M. Selvaggi, Z. Staykova, H. Van Haevermaet, P. Van Mechelen, N. Van Remortel, A. Van Spillbeeck

Vrije Universiteit Brussel, Brussel, Belgium

F. Blekman, S. Blyweert, J. D'Hondt, R. Gonzalez Suarez, A. Kalogeropoulos, M. Maes, A. Olbrechts, W. Van Doninck, P. Van Mulders, G.P. Van Onsem, I. Villella

Université Libre de Bruxelles, Bruxelles, Belgium

B. Clerbaux, G. De Lentdecker, V. Dero, A.P.R. Gay, T. Hreus, A. Léonard, P.E. Marage, A. Mohammadi, T. Reis, L. Thomas, G. Vander Marcken, C. Vander Velde, P. Vanlaer, J. Wang

Ghent University, Ghent, Belgium

V. Adler, K. Beernaert, A. Cimmino, S. Costantini, G. Garcia, M. Grunewald, B. Klein, J. Lellouch, A. Marinov, J. McCartin, A.A. Ocampo Rios, D. Ryckbosch, N. Strobbe, F. Thyssen, M. Tytgat, P. Verwilligen, S. Walsh, E. Yazgan, N. Zaganidis

Université Catholique de Louvain, Louvain-la-Neuve, Belgium

S. Basegmez, G. Bruno, R. Castello, L. Ceard, C. Delaere, T. du Pree, D. Favart, L. Forthomme, A. Giammanco², J. Hollar, V. Lemaitre, J. Liao, O. Militaru, C. Nuttens, D. Pagano, A. Pin, K. Piotrkowski, N. Schul, J.M. Vizan Garcia

Université de Mons, Mons, Belgium

N. Belyi, T. Caebergs, E. Daubie, G.H. Hammad

Centro Brasileiro de Pesquisas Fisicas, Rio de Janeiro, Brazil

G.A. Alves, M. Correa Martins Junior, D. De Jesus Damiao, T. Martins, M.E. Pol, M.H.G. Souza

Universidade do Estado do Rio de Janeiro, Rio de Janeiro, Brazil

W.L. Aldá Júnior, W. Carvalho, A. Custódio, E.M. Da Costa, C. De Oliveira Martins, S. Fonseca De Souza, D. Matos Figueiredo, L. Mundim, H. Nogima, V. Oguri, W.L. Prado Da Silva, A. Santoro, L. Soares Jorge, A. Sznajder

Instituto de Fisica Teorica, Universidade Estadual Paulista, Sao Paulo, Brazil

T.S. Anjos³, C.A. Bernardes³, F.A. Dias⁴, T.R. Fernandez Perez Tomei, E.M. Gregores³, C. Lagana, F. Marinho, P.G. Mercadante³, S.F. Novaes, Sandra S. Padula

Institute for Nuclear Research and Nuclear Energy, Sofia, Bulgaria

V. Genchev⁵, P. Iaydjiev⁵, S. Piperov, M. Rodozov, S. Stoykova, G. Sultanov, V. Tcholakov, R. Trayanov, M. Vutova

University of Sofia, Sofia, Bulgaria

A. Dimitrov, R. Hadjiiska, V. Kozhuharov, L. Litov, B. Pavlov, P. Petkov

Institute of High Energy Physics, Beijing, China

J.G. Bian, G.M. Chen, H.S. Chen, C.H. Jiang, D. Liang, S. Liang, X. Meng, J. Tao, J. Wang, X. Wang, Z. Wang, H. Xiao, M. Xu, J. Zang, Z. Zhang

State Key Lab. of Nucl. Phys. and Tech., Peking University, Beijing, China

C. Asawatangtrakuldee, Y. Ban, Y. Guo, W. Li, S. Liu, Y. Mao, S.J. Qian, H. Teng, D. Wang, L. Zhang, W. Zou

Universidad de Los Andes, Bogota, Colombia

C. Avila, J.P. Gomez, B. Gomez Moreno, A.F. Osorio Oliveros, J.C. Sanabria

Technical University of Split, Split, Croatia

N. Godinovic, D. Lelas, R. Plestina⁶, D. Polic, I. Puljak⁵

University of Split, Split, Croatia

Z. Antunovic, M. Kovac

Institute Rudjer Boskovic, Zagreb, Croatia

V. Brigljevic, S. Duric, K. Kadija, J. Luetic, S. Morovic

University of Cyprus, Nicosia, Cyprus

A. Attikis, M. Galanti, G. Mavromanolakis, J. Mousa, C. Nicolaou, F. Ptochos, P.A. Razis

Charles University, Prague, Czech Republic

M. Finger, M. Finger Jr.

Academy of Scientific Research and Technology of the Arab Republic of Egypt, Egyptian Network of High Energy Physics, Cairo, Egypt

Y. Assran⁷, S. Elgammal⁸, A. Ellithi Kamel⁹, S. Khalil⁸, M.A. Mahmoud¹⁰, A. Radi^{11,12}

National Institute of Chemical Physics and Biophysics, Tallinn, Estonia

M. Kadastik, M. Müntel, M. Raidal, L. Rebane, A. Tiko

Department of Physics, University of Helsinki, Helsinki, Finland

P. Eerola, G. Fedi, M. Voutilainen

Helsinki Institute of Physics, Helsinki, Finland

J. Härkönen, A. Heikkinen, V. Karimäki, R. Kinnunen, M.J. Kortelainen, T. Lampén, K. Lassila-Perini, S. Lehti, T. Lindén, P. Luukka, T. Mäenpää, T. Peltola, E. Tuominen, J. Tuominiemi, E. Tuovinen, D. Ungaro, L. Wendland

Lappeenranta University of Technology, Lappeenranta, Finland

K. Banzuzi, A. Karjalainen, A. Korpela, T. Tuuva

DSM/IRFU, CEA/Saclay, Gif-sur-Yvette, France

M. Besancon, S. Choudhury, M. Dejardin, D. Denegri, B. Fabbro, J.L. Faure, F. Ferri, S. Ganjour, A. Givernaud, P. Gras, G. Hamel de Monchenault, P. Jarry, E. Locci, J. Malcles, L. Millischer, A. Nayak, J. Rander, A. Rosowsky, I. Shreyber, M. Titov

Laboratoire Leprince-Ringuet, Ecole Polytechnique, IN2P3-CNRS, Palaiseau, France

S. Baffioni, F. Beaudette, L. Benhabib, L. Bianchini, M. Bluj¹³, C. Broutin, P. Busson, C. Charlot, N. Daci, T. Dahms, L. Dobrzynski, R. Granier de Cassagnac, M. Haguenaue, P. Miné, C. Mironov, I.N. Naranjo, M. Nguyen, C. Ochando, P. Paganini, D. Sabes, R. Salerno, Y. Sirois, C. Veelken, A. Zabi

Institut Pluridisciplinaire Hubert Curien, Université de Strasbourg, Université de Haute Alsace Mulhouse, CNRS/IN2P3, Strasbourg, France

J.-L. Agram¹⁴, J. Andrea, D. Bloch, D. Bodin, J.-M. Brom, M. Cardaci, E.C. Chabert, C. Collard, E. Conte¹⁴, F. Drouhin¹⁴, C. Ferro, J.-C. Fontaine¹⁴, D. Gelé, U. Goerlach, P. Juillot, A.-C. Le Bihan, P. Van Hove

Centre de Calcul de l'Institut National de Physique Nucleaire et de Physique des Particules, CNRS/IN2P3, Villeurbanne, France, Villeurbanne, France

F. Fassi, D. Mercier

Université de Lyon, Université Claude Bernard Lyon 1, CNRS-IN2P3, Institut de Physique Nucléaire de Lyon, Villeurbanne, France

S. Beauceron, N. Beaupere, O. Bondu, G. Boudoul, J. Chasserat, R. Chierici⁵, D. Contardo, P. Depasse, H. El Mamouni, J. Fay, S. Gascon, M. Gouzevitch, B. Ille, T. Kurca, M. Lethuillier, L. Mirabito, S. Perries, L. Sgandurra, V. Sordini, Y. Tschudi, P. Verdier, S. Viret

Institute of High Energy Physics and Informatization, Tbilisi State University, Tbilisi, Georgia

Z. Tsamalaidze¹⁵

RWTH Aachen University, I. Physikalisches Institut, Aachen, Germany

G. Anagnostou, C. Autermann, S. Beranek, M. Edelhoff, L. Feld, N. Heracleous, O. Hindrichs, R. Jussen, K. Klein, J. Merz, A. Ostapchuk, A. Perieanu, F. Raupach, J. Sammet, S. Schael, D. Sprenger, H. Weber, B. Wittmer, V. Zhukov¹⁶

RWTH Aachen University, III. Physikalisches Institut A, Aachen, Germany

M. Ata, J. Caudron, E. Dietz-Laursonn, D. Duchardt, M. Erdmann, R. Fischer, A. Güth, T. Hebbeker, C. Heidemann, K. Hoepfner, D. Klingebiel, P. Kreuzer, M. Merschmeyer, A. Meyer, M. Olschewski, P. Papacz, H. Pieta, H. Reithler, S.A. Schmitz, L. Sonnenschein, J. Steggemann, D. Teyssier, M. Weber

RWTH Aachen University, III. Physikalisches Institut B, Aachen, Germany

M. Bontenackels, V. Cherepanov, Y. Erdogan, G. Flügge, H. Geenen, M. Geisler, W. Haj Ahmad, F. Hoehle, B. Kargoll, T. Kress, Y. Kuessel, J. Lingemann⁵, A. Nowack, L. Perchalla, O. Pooth, P. Sauerland, A. Stahl

Deutsches Elektronen-Synchrotron, Hamburg, Germany

M. Aldaya Martin, J. Behr, W. Behrenhoff, U. Behrens, M. Bergholz¹⁷, A. Bethani, K. Borras, A. Burgmeier, A. Cakir, L. Calligaris, A. Campbell, E. Castro, F. Costanza, D. Dammann, C. Diez Pardos, G. Eckerlin, D. Eckstein, G. Flucke, A. Geiser, I. Glushkov, P. Gunnellini, S. Habib, J. Hauk, G. Hellwig, H. Jung, M. Kasemann, P. Katsas, C. Kleinwort, H. Kluge, A. Knutsson, M. Krämer, D. Krücker, E. Kuznetsova, W. Lange, W. Lohmann¹⁷, B. Lutz, R. Mankel, I. Marfin, M. Marienfeld, I.-A. Melzer-Pellmann, A.B. Meyer, J. Mnich, A. Mussgiller, S. Naumann-Emme, O. Novgorodova, J. Olzem, H. Perrey, A. Petrukhin, D. Pitzl, A. Raspereza, P.M. Ribeiro Cipriano, C. Riedl, E. Ron, M. Rosin, J. Salfeld-Nebgen, R. Schmidt¹⁷, T. Schoerner-Sadenius, N. Sen, A. Spiridonov, M. Stein, R. Walsh, C. Wissing

University of Hamburg, Hamburg, Germany

V. Blobel, J. Draeger, H. Enderle, J. Erfle, U. Gebbert, M. Görner, T. Hermanns, R.S. Höing, K. Kaschube, G. Kaussen, H. Kirschenmann, R. Klanner, J. Lange, B. Mura, F. Nowak, T. Peiffer, N. Pietsch, D. Rathjens, C. Sander, H. Schettler, P. Schleper, E. Schlieckau, A. Schmidt, M. Schröder, T. Schum, M. Seidel, V. Sola, H. Stadie, G. Steinbrück, J. Thomsen, L. Vanelderen

Institut für Experimentelle Kernphysik, Karlsruhe, Germany

C. Barth, J. Berger, C. Böser, T. Chwalek, W. De Boer, A. Descroix, A. Dierlamm, M. Feindt, M. Guthoff⁵, C. Hackstein, F. Hartmann, T. Hauth⁵, M. Heinrich, H. Held, K.H. Hoffmann, U. Husemann, I. Katkov¹⁶, J.R. Komaragiri, P. Lobelle Pardo, D. Martschei, S. Mueller, Th. Müller, M. Niegel, A. Nürnberg, O. Oberst, A. Oehler, J. Ott, G. Quast, K. Rabbertz, F. Ratnikov, N. Ratnikova, S. Röcker, F.-P. Schilling, G. Schott, H.J. Simonis, F.M. Stober, D. Troendle, R. Ulrich, J. Wagner-Kuhr, S. Wayand, T. Weiler, M. Zeise

Institute of Nuclear Physics "Demokritos", Aghia Paraskevi, Greece

G. Daskalakis, T. Gerasis, S. Kesisoglou, A. Kyriakis, D. Loukas, I. Manolakos, A. Markou, C. Markou, C. Mavrommatis, E. Ntomari

University of Athens, Athens, Greece

L. Gouskos, T.J. Mertzimekis, A. Panagiotou, N. Saoulidou

University of Ioánnina, Ioánnina, Greece

I. Evangelou, C. Foudas, P. Kokkas, N. Manthos, I. Papadopoulos, V. Patras

KFKI Research Institute for Particle and Nuclear Physics, Budapest, Hungary

G. Bencze, C. Hajdu, P. Hidas, D. Horvath¹⁸, F. Sikler, V. Veszpremi, G. Vesztergombi¹⁹

Institute of Nuclear Research ATOMKI, Debrecen, Hungary

N. Beni, S. Czellar, J. Molnar, J. Palinkas, Z. Szillasi

University of Debrecen, Debrecen, Hungary

J. Karancsi, P. Raics, Z.L. Trocsanyi, B. Ujvari

Panjab University, Chandigarh, India

S.B. Beri, V. Bhatnagar, N. Dhingra, R. Gupta, M. Kaur, M.Z. Mehta, N. Nishu, L.K. Saini, A. Sharma, J.B. Singh

University of Delhi, Delhi, India

Ashok Kumar, Arun Kumar, S. Ahuja, A. Bhardwaj, B.C. Choudhary, S. Malhotra, M. Naimuddin, K. Ranjan, V. Sharma, R.K. Shivpuri

Saha Institute of Nuclear Physics, Kolkata, India

S. Banerjee, S. Bhattacharya, S. Dutta, B. Gomber, Sa. Jain, Sh. Jain, R. Khurana, S. Sarkar, M. Sharan

Bhabha Atomic Research Centre, Mumbai, India

A. Abdulsalam, R.K. Choudhury, D. Dutta, S. Kailas, V. Kumar, P. Mehta, A.K. Mohanty⁵, L.M. Pant, P. Shukla

Tata Institute of Fundamental Research - EHEP, Mumbai, India

T. Aziz, S. Ganguly, M. Guchait²⁰, M. Maity²¹, G. Majumder, K. Mazumdar, G.B. Mohanty, B. Parida, K. Sudhakar, N. Wickramage

Tata Institute of Fundamental Research - HECR, Mumbai, India

S. Banerjee, S. Dugad

Institute for Research in Fundamental Sciences (IPM), Tehran, Iran

H. Arfaei²², H. Bakhshiansohi, S.M. Etesami²³, A. Fahim²², M. Hashemi, H. Hesari, A. Jafari, M. Khakzad, M. Mohammadi Najafabadi, S. Paktinat Mehdiabadi, B. Safarzadeh²⁴, M. Zeinali

INFN Sezione di Bari ^a, Università di Bari ^b, Politecnico di Bari ^c, Bari, Italy

M. Abbrescia^{a,b}, L. Barbone^{a,b}, C. Calabria^{a,b,5}, S.S. Chhibra^{a,b}, A. Colaleo^a, D. Creanza^{a,c},

N. De Filippis^{a,c,5}, M. De Palma^{a,b}, L. Fiore^a, G. Iaselli^{a,c}, L. Lusito^{a,b}, G. Maggi^{a,c}, M. Maggi^a, B. Marangelli^{a,b}, S. My^{a,c}, S. Nuzzo^{a,b}, N. Pacifico^{a,b}, A. Pompili^{a,b}, G. Pugliese^{a,c}, G. Selvaggi^{a,b}, L. Silvestris^a, G. Singh^{a,b}, R. Venditti^{a,b}, G. Zito^a

INFN Sezione di Bologna ^a, Università di Bologna ^b, Bologna, Italy

G. Abbiendi^a, A.C. Benvenuti^a, D. Bonacorsi^{a,b}, S. Braibant-Giacomelli^{a,b}, L. Brigliadori^{a,b}, P. Capiluppi^{a,b}, A. Castro^{a,b}, F.R. Cavallo^a, M. Cuffiani^{a,b}, G.M. Dallavalle^a, F. Fabbri^a, A. Fanfani^{a,b}, D. Fasanella^{a,b,5}, P. Giacomelli^a, C. Grandi^a, L. Guiducci^{a,b}, S. Marcellini^a, G. Masetti^a, M. Meneghelli^{a,b,5}, A. Montanari^a, F.L. Navarria^{a,b}, F. Odorici^a, A. Perrotta^a, F. Primavera^{a,b}, A.M. Rossi^{a,b}, T. Rovelli^{a,b}, G.P. Siroli^{a,b}, R. Travaglini^{a,b}

INFN Sezione di Catania ^a, Università di Catania ^b, Catania, Italy

S. Albergo^{a,b}, G. Cappello^{a,b}, M. Chiorboli^{a,b}, S. Costa^{a,b}, R. Potenza^{a,b}, A. Tricomi^{a,b}, C. Tuve^{a,b}

INFN Sezione di Firenze ^a, Università di Firenze ^b, Firenze, Italy

G. Barbagli^a, V. Ciulli^{a,b}, C. Civinini^a, R. D'Alessandro^{a,b}, E. Focardi^{a,b}, S. Frosali^{a,b}, E. Gallo^a, S. Gonzi^{a,b}, M. Meschini^a, S. Paoletti^a, G. Sguazzoni^a, A. Tropiano^{a,b}

INFN Laboratori Nazionali di Frascati, Frascati, Italy

L. Benussi, S. Bianco, S. Colafranceschi²⁵, F. Fabbri, D. Piccolo

INFN Sezione di Genova ^a, Università di Genova ^b, Genova, Italy

P. Fabbricatore^a, R. Musenich^a, S. Tosi^{a,b}

INFN Sezione di Milano-Bicocca ^a, Università di Milano-Bicocca ^b, Milano, Italy

A. Benaglia^{a,b}, F. De Guio^{a,b}, L. Di Matteo^{a,b,5}, S. Fiorendi^{a,b}, S. Gennai^{a,5}, A. Ghezzi^{a,b}, S. Malvezzi^a, R.A. Manzoni^{a,b}, A. Martelli^{a,b}, A. Massironi^{a,b,5}, D. Menasce^a, L. Moroni^a, M. Paganoni^{a,b}, D. Pedrini^a, S. Ragazzi^{a,b}, N. Redaelli^a, S. Sala^a, T. Tabarelli de Fatis^{a,b}

INFN Sezione di Napoli ^a, Università di Napoli "Federico II" ^b, Napoli, Italy

S. Buontempo^a, C.A. Carrillo Montoya^a, N. Cavallo^{a,26}, A. De Cosa^{a,b,5}, O. Dogangun^{a,b}, F. Fabozzi^{a,26}, A.O.M. Iorio^{a,b}, L. Lista^a, S. Meola^{a,27}, M. Merola^{a,b}, P. Paolucci^{a,5}

INFN Sezione di Padova ^a, Università di Padova ^b, Università di Trento (Trento) ^c, Padova, Italy

P. Azzi^a, N. Bacchetta^{a,5}, P. Bellan^{a,b}, D. Bisello^{a,b}, A. Branca^{a,b,5}, R. Carlin^{a,b}, P. Checchia^a, T. Dorigo^a, U. Dosselli^a, F. Gasparini^{a,b}, U. Gasparini^{a,b}, A. Gozzelino^a, K. Kanishchev^{a,c}, S. Lacaprara^a, I. Lazzizzera^{a,c}, M. Margoni^{a,b}, A.T. Meneguzzo^{a,b}, M. Nespolo^{a,5}, J. Pazzini^{a,b}, P. Ronchese^{a,b}, F. Simonetto^{a,b}, E. Torassa^a, S. Vanini^{a,b}, P. Zotto^{a,b}, G. Zumerle^{a,b}

INFN Sezione di Pavia ^a, Università di Pavia ^b, Pavia, Italy

M. Gabusi^{a,b}, S.P. Ratti^{a,b}, C. Riccardi^{a,b}, P. Torre^{a,b}, P. Vitulo^{a,b}

INFN Sezione di Perugia ^a, Università di Perugia ^b, Perugia, Italy

M. Biasini^{a,b}, G.M. Bilei^a, L. Fanò^{a,b}, P. Lariccia^{a,b}, G. Mantovani^{a,b}, M. Menichelli^a, A. Nappi^{a,b†}, F. Romeo^{a,b}, A. Saha^a, A. Santocchia^{a,b}, A. Spiezia^{a,b}, S. Taroni^{a,b}

INFN Sezione di Pisa ^a, Università di Pisa ^b, Scuola Normale Superiore di Pisa ^c, Pisa, Italy

P. Azzurri^{a,c}, G. Bagliesi^a, T. Boccali^a, G. Broccolo^{a,c}, R. Castaldi^a, R.T. D'Agnolo^{a,c,5}, R. Dell'Orso^a, F. Fiori^{a,b,5}, L. Foà^{a,c}, A. Giassi^a, A. Kraan^a, F. Ligabue^{a,c}, T. Lomtadze^a, L. Martini^{a,28}, A. Messineo^{a,b}, F. Palla^a, A. Rizzi^{a,b}, A.T. Serban^{a,29}, P. Spagnolo^a, P. Squillacioti^{a,5}, R. Tenchini^a, G. Tonelli^{a,b}, A. Venturi^a, P.G. Verdini^a

INFN Sezione di Roma ^a, Università di Roma ^b, Roma, Italy

L. Barone^{a,b}, F. Cavallari^a, D. Del Re^{a,b}, M. Diemoz^a, C. Fanelli^{a,b}, M. Grassi^{a,b,5}, E. Longo^{a,b}

P. Meridiani^{a,5}, F. Micheli^{a,b}, S. Nourbakhsh^{a,b}, G. Organtini^{a,b}, R. Paramatti^a, S. Rahatlou^{a,b}, M. Sigamani^a, L. Soffi^{a,b}

INFN Sezione di Torino^a, Università di Torino^b, Università del Piemonte Orientale (Novara)^c, Torino, Italy

N. Amapane^{a,b}, R. Arcidiacono^{a,c}, S. Argiro^{a,b}, M. Arneodo^{a,c}, C. Biino^a, N. Cartiglia^a, M. Costa^{a,b}, N. Demaria^a, C. Mariotti^{a,5}, S. Maselli^a, E. Migliore^{a,b}, V. Monaco^{a,b}, M. Musich^{a,5}, M.M. Obertino^{a,c}, N. Pastrone^a, M. Pelliccioni^a, A. Potenza^{a,b}, A. Romero^{a,b}, M. Ruspa^{a,c}, R. Sacchi^{a,b}, A. Solano^{a,b}, A. Staiano^a, A. Vilela Pereira^a

INFN Sezione di Trieste^a, Università di Trieste^b, Trieste, Italy

S. Belforte^a, V. Candolise^{a,b}, M. Casarsa^a, F. Cossutti^a, G. Della Ricca^{a,b}, B. Gobbo^a, M. Marone^{a,b,5}, D. Montanino^{a,b,5}, A. Penzo^a, A. Schizzi^{a,b}

Kangwon National University, Chunchon, Korea

S.G. Heo, T.Y. Kim, S.K. Nam

Kyungpook National University, Daegu, Korea

S. Chang, D.H. Kim, G.N. Kim, D.J. Kong, H. Park, S.R. Ro, D.C. Son, T. Son

Chonnam National University, Institute for Universe and Elementary Particles, Kwangju, Korea

J.Y. Kim, Zero J. Kim, S. Song

Korea University, Seoul, Korea

S. Choi, D. Gyun, B. Hong, M. Jo, H. Kim, T.J. Kim, K.S. Lee, D.H. Moon, S.K. Park

University of Seoul, Seoul, Korea

M. Choi, J.H. Kim, C. Park, I.C. Park, S. Park, G. Ryu

Sungkyunkwan University, Suwon, Korea

Y. Cho, Y. Choi, Y.K. Choi, J. Goh, M.S. Kim, E. Kwon, B. Lee, J. Lee, S. Lee, H. Seo, I. Yu

Vilnius University, Vilnius, Lithuania

M.J. Bilinskas, I. Grigelionis, M. Janulis, A. Juodagalvis

Centro de Investigacion y de Estudios Avanzados del IPN, Mexico City, Mexico

H. Castilla-Valdez, E. De La Cruz-Burelo, I. Heredia-de La Cruz, R. Lopez-Fernandez, R. Magaña Villalba, J. Martínez-Ortega, A. Sánchez-Hernández, L.M. Villasenor-Cendejas

Universidad Iberoamericana, Mexico City, Mexico

S. Carrillo Moreno, F. Vazquez Valencia

Benemerita Universidad Autonoma de Puebla, Puebla, Mexico

H.A. Salazar Ibarguen

Universidad Autónoma de San Luis Potosí, San Luis Potosí, Mexico

E. Casimiro Linares, A. Morelos Pineda, M.A. Reyes-Santos

University of Auckland, Auckland, New Zealand

D. Krofcheck

University of Canterbury, Christchurch, New Zealand

A.J. Bell, P.H. Butler, R. Doesburg, S. Reucroft, H. Silverwood

National Centre for Physics, Quaid-I-Azam University, Islamabad, Pakistan

M. Ahmad, M.H. Ansari, M.I. Asghar, H.R. Hoorani, S. Khalid, W.A. Khan, T. Khurshid, S. Qazi, M.A. Shah, M. Shoaib

National Centre for Nuclear Research, Swierk, Poland

H. Bialkowska, B. Boimska, T. Frueboes, R. Gokieli, M. Górski, M. Kazana, K. Nawrocki, K. Romanowska-Rybinska, M. Szleper, G. Wrochna, P. Zalewski

Institute of Experimental Physics, Faculty of Physics, University of Warsaw, Warsaw, Poland

G. Brona, K. Bunkowski, M. Cwiok, W. Dominik, K. Doroba, A. Kalinowski, M. Konecki, J. Krolikowski

Laboratório de Instrumentação e Física Experimental de Partículas, Lisboa, Portugal

N. Almeida, P. Bargassa, A. David, P. Faccioli, P.G. Ferreira Parracho, M. Gallinaro, J. Seixas, J. Varela, P. Vischia

Joint Institute for Nuclear Research, Dubna, Russia

I. Belotelov, P. Bunin, M. Gavrilenko, I. Golutvin, I. Gorbunov, A. Kamenev, V. Karjavin, G. Kozlov, A. Lanev, A. Malakhov, P. Moisenz, V. Palichik, V. Perelygin, S. Shmatov, V. Smirnov, A. Volodko, A. Zarubin

Petersburg Nuclear Physics Institute, Gatchina (St. Petersburg), Russia

S. Evstyukhin, V. Golovtsov, Y. Ivanov, V. Kim, P. Levchenko, V. Murzin, V. Oreshkin, I. Smirnov, V. Sulimov, L. Uvarov, S. Vavilov, A. Vorobyev, An. Vorobyev

Institute for Nuclear Research, Moscow, Russia

Yu. Andreev, A. Dermenev, S. Gninenko, N. Golubev, M. Kirsanov, N. Krasnikov, V. Matveev, A. Pashenkov, D. Tlisov, A. Toropin

Institute for Theoretical and Experimental Physics, Moscow, Russia

V. Epshteyn, M. Erofeeva, V. Gavrilo, M. Kossov, N. Lychkovskaya, V. Popov, G. Safronov, S. Semenov, V. Stolin, E. Vlasov, A. Zhokin

Moscow State University, Moscow, Russia

A. Belyaev, E. Boos, M. Dubinin⁴, L. Dudko, A. Ershov, A. Gribushin, V. Klyukhin, O. Kodolova, I. Lokhtin, A. Markina, S. Obraztsov, M. Perfilov, S. Petrushanko, A. Popov, L. Sarycheva[†], V. Savrin, A. Snigirev

P.N. Lebedev Physical Institute, Moscow, Russia

V. Andreev, M. Azarkin, I. Dremin, M. Kirakosyan, A. Leonidov, G. Mesyats, S.V. Rusakov, A. Vinogradov

State Research Center of Russian Federation, Institute for High Energy Physics, Protvino, Russia

I. Azhgirey, I. Bayshev, S. Bitioukov, V. Grishin⁵, V. Kachanov, D. Konstantinov, V. Krychkine, V. Petrov, R. Ryutin, A. Sobol, L. Tourtchanovitch, S. Troshin, N. Tyurin, A. Uzunian, A. Volkov

University of Belgrade, Faculty of Physics and Vinca Institute of Nuclear Sciences, Belgrade, Serbia

P. Adzic³⁰, M. Djordjevic, M. Ekmedzic, D. Krpic³⁰, J. Milosevic

Centro de Investigaciones Energéticas Medioambientales y Tecnológicas (CIEMAT), Madrid, Spain

M. Aguilar-Benitez, J. Alcaraz Maestre, P. Arce, C. Battilana, E. Calvo, M. Cerrada, M. Chamizo Llatas, N. Colino, B. De La Cruz, A. Delgado Peris, D. Domínguez Vázquez, C. Fernandez

Bedoya, J.P. Fernández Ramos, A. Ferrando, J. Flix, M.C. Fouz, P. Garcia-Abia, O. Gonzalez Lopez, S. Goy Lopez, J.M. Hernandez, M.I. Josa, G. Merino, J. Puerta Pelayo, A. Quintario Olmeda, I. Redondo, L. Romero, J. Santaolalla, M.S. Soares, C. Willmott

Universidad Autónoma de Madrid, Madrid, Spain

C. Albajar, G. Codispoti, J.F. de Trocóniz

Universidad de Oviedo, Oviedo, Spain

H. Brun, J. Cuevas, J. Fernandez Menendez, S. Folgueras, I. Gonzalez Caballero, L. Lloret Iglesias, J. Piedra Gomez

Instituto de Física de Cantabria (IFCA), CSIC-Universidad de Cantabria, Santander, Spain

J.A. Brochero Cifuentes, I.J. Cabrillo, A. Calderon, S.H. Chuang, J. Duarte Campderros, M. Felcini³¹, M. Fernandez, G. Gomez, J. Gonzalez Sanchez, A. Graziano, C. Jorda, A. Lopez Virto, J. Marco, R. Marco, C. Martinez Rivero, F. Matorras, F.J. Munoz Sanchez, T. Rodrigo, A.Y. Rodríguez-Marrero, A. Ruiz-Jimeno, L. Scodellaro, I. Vila, R. Vilar Cortabitarte

CERN, European Organization for Nuclear Research, Geneva, Switzerland

D. Abbaneo, E. Auffray, G. Auzinger, M. Bachtis, P. Baillon, A.H. Ball, D. Barney, J.F. Benitez, C. Bernet⁶, G. Bianchi, P. Bloch, A. Bocci, A. Bonato, C. Botta, H. Breuker, T. Camporesi, G. Cerminara, T. Christiansen, J.A. Coarasa Perez, D. D'Enterria, A. Dabrowski, A. De Roeck, S. Di Guida, M. Dobson, N. Dupont-Sagorin, A. Elliott-Peisert, B. Frisch, W. Funk, G. Georgiou, M. Giffels, D. Gigi, K. Gill, D. Giordano, M. Girone, M. Giunta, F. Glege, R. Gomez-Reino Garrido, P. Govoni, S. Gowdy, R. Guida, M. Hansen, P. Harris, C. Hartl, J. Harvey, B. Hegner, A. Hinzmann, V. Innocente, P. Janot, K. Kaadze, E. Karavakis, K. Kousouris, P. Lecoq, Y.-J. Lee, P. Lenzi, C. Lourenço, N. Magini, T. Mäki, M. Malberti, L. Malgeri, M. Mannelli, L. Masetti, F. Meijers, S. Mersi, E. Meschi, R. Moser, M.U. Mozer, M. Mulders, P. Musella, E. Nesvold, T. Orimoto, L. Orsini, E. Palencia Cortezon, E. Perez, L. Perrozzi, A. Petrilli, A. Pfeiffer, M. Pierini, M. Pimiä, D. Piparo, G. Polese, L. Quertenmont, A. Racz, W. Reece, J. Rodrigues Antunes, G. Rolandi³², C. Rovelli³³, M. Rovere, H. Sakulin, F. Santanastasio, C. Schäfer, C. Schwick, I. Segoni, S. Sekmen, A. Sharma, P. Siegrist, P. Silva, M. Simon, P. Sphicas³⁴, D. Spiga, A. Tsiros, G.I. Veres¹⁹, J.R. Vlimant, H.K. Wöhri, S.D. Worm³⁵, W.D. Zeuner

Paul Scherrer Institut, Villigen, Switzerland

W. Bertl, K. Deiters, W. Erdmann, K. Gabathuler, R. Horisberger, Q. Ingram, H.C. Kaestli, S. König, D. Kotlinski, U. Langenegger, F. Meier, D. Renker, T. Rohe, J. Sibille³⁶

Institute for Particle Physics, ETH Zurich, Zurich, Switzerland

L. Bäni, P. Bortignon, M.A. Buchmann, B. Casal, N. Chanon, A. Deisher, G. Dissertori, M. Dittmar, M. Donegà, M. Dünser, J. Eugster, K. Freudenreich, C. Grab, D. Hits, P. Lecomte, W. Lustermann, A.C. Marini, P. Martinez Ruiz del Arbol, N. Mohr, F. Moortgat, C. Nägeli³⁷, P. Nef, F. Nessi-Tedaldi, F. Pandolfi, L. Pape, F. Pauss, M. Peruzzi, F.J. Ronga, M. Rossini, L. Sala, A.K. Sanchez, A. Starodumov³⁸, B. Stieger, M. Takahashi, L. Tauscher[†], A. Thea, K. Theofilatos, D. Treille, C. Urscheler, R. Wallny, H.A. Weber, L. Wehrli

Universität Zürich, Zurich, Switzerland

C. Amsler, V. Chiochia, S. De Visscher, C. Favaro, M. Ivova Rikova, B. Millan Mejias, P. Otiougova, P. Robmann, H. Snoek, S. Tuppen, M. Verzetti

National Central University, Chung-Li, Taiwan

Y.H. Chang, K.H. Chen, C.M. Kuo, S.W. Li, W. Lin, Z.K. Liu, Y.J. Lu, D. Mekterovic, A.P. Singh, R. Volpe, S.S. Yu

National Taiwan University (NTU), Taipei, Taiwan

P. Bartalini, P. Chang, Y.H. Chang, Y.W. Chang, Y. Chao, K.F. Chen, C. Dietz, U. Grundler, W.-S. Hou, Y. Hsiung, K.Y. Kao, Y.J. Lei, R.-S. Lu, D. Majumder, E. Petrakou, X. Shi, J.G. Shiu, Y.M. Tzeng, X. Wan, M. Wang

Chulalongkorn University, Bangkok, Thailand

B. Asavapibhop, N. Srimanobhas

Cukurova University, Adana, Turkey

A. Adiguzel, M.N. Bakirci³⁹, S. Cerci⁴⁰, C. Dozen, I. Dumanoglu, E. Eskut, S. Girgis, G. Gokbulut, E. Gurpinar, I. Hos, E.E. Kangal, T. Karaman, G. Karapinar⁴¹, A. Kayis Topaksu, G. Onengut, K. Ozdemir, S. Ozturk⁴², A. Polatoz, K. Sogut⁴³, D. Sunar Cerci⁴⁰, B. Tali⁴⁰, H. Topakli³⁹, L.N. Vergili, M. Vergili

Middle East Technical University, Physics Department, Ankara, Turkey

I.V. Akin, T. Aliev, B. Bilin, S. Bilmis, M. Deniz, H. Gamsizkan, A.M. Guler, K. Ocalan, A. Ozpineci, M. Serin, R. Sever, U.E. Surat, M. Yalvac, E. Yildirim, M. Zeyrek

Bogazici University, Istanbul, Turkey

E. Gülmez, B. Isildak⁴⁴, M. Kaya⁴⁵, O. Kaya⁴⁵, S. Ozkorucuklu⁴⁶, N. Sonmez⁴⁷

Istanbul Technical University, Istanbul, Turkey

K. Cankocak

National Scientific Center, Kharkov Institute of Physics and Technology, Kharkov, Ukraine

L. Levchuk

University of Bristol, Bristol, United Kingdom

F. Bostock, J.J. Brooke, E. Clement, D. Cussans, H. Flacher, R. Frazier, J. Goldstein, M. Grimes, G.P. Heath, H.F. Heath, L. Kreczko, S. Metson, D.M. Newbold³⁵, K. Nirunpong, A. Poll, S. Senkin, V.J. Smith, T. Williams

Rutherford Appleton Laboratory, Didcot, United Kingdom

L. Basso⁴⁸, K.W. Bell, A. Belyaev⁴⁸, C. Brew, R.M. Brown, D.J.A. Cockerill, J.A. Coughlan, K. Harder, S. Harper, J. Jackson, B.W. Kennedy, E. Olaiya, D. Petyt, B.C. Radburn-Smith, C.H. Shepherd-Themistocleous, I.R. Tomalin, W.J. Womersley

Imperial College, London, United Kingdom

R. Bainbridge, G. Ball, R. Beuselinck, O. Buchmuller, D. Colling, N. Cripps, M. Cutajar, P. Dauncey, G. Davies, M. Della Negra, W. Ferguson, J. Fulcher, D. Futyan, A. Gilbert, A. Guneratne Bryer, G. Hall, Z. Hatherell, J. Hays, G. Iles, M. Jarvis, G. Karapostoli, L. Lyons, A.-M. Magnan, J. Marrouche, B. Mathias, R. Nandi, J. Nash, A. Nikitenko³⁸, A. Papageorgiou, J. Pela, M. Pesaresi, K. Petridis, M. Pioppi⁴⁹, D.M. Raymond, S. Rogerson, A. Rose, M.J. Ryan, C. Seez, P. Sharp[†], A. Sparrow, M. Stoye, A. Tapper, M. Vazquez Acosta, T. Virdee, S. Wakefield, N. Wardle, T. Whyntie

Brunel University, Uxbridge, United Kingdom

M. Chadwick, J.E. Cole, P.R. Hobson, A. Khan, P. Kyberd, D. Leggat, D. Leslie, W. Martin, I.D. Reid, P. Symonds, L. Teodorescu, M. Turner

Baylor University, Waco, USA

K. Hatakeyama, H. Liu, T. Scarborough

The University of Alabama, Tuscaloosa, USA

O. Charaf, C. Henderson, P. Rumerio

Boston University, Boston, USA

A. Avetisyan, T. Bose, C. Fantasia, A. Heister, J. St. John, P. Lawson, D. Lazic, J. Rohlf, D. Sperka, L. Sulak

Brown University, Providence, USA

J. Alimena, S. Bhattacharya, D. Cutts, Z. Demiragli, A. Ferapontov, U. Heintz, S. Jabeen, G. Kukartsev, E. Laird, G. Landsberg, M. Luk, M. Narain, D. Nguyen, M. Segala, T. Sinthuprasith, T. Speer, K.V. Tsang

University of California, Davis, Davis, USA

R. Breedon, G. Breto, M. Calderon De La Barca Sanchez, S. Chauhan, M. Chertok, J. Conway, R. Conway, P.T. Cox, J. Dolen, R. Erbacher, M. Gardner, R. Houtz, W. Ko, A. Kopecky, R. Lander, O. Mall, T. Miceli, D. Pellett, F. Ricci-tam, B. Rutherford, M. Searle, J. Smith, M. Squires, M. Tripathi, R. Vasquez Sierra, R. Yohay

University of California, Los Angeles, Los Angeles, USA

V. Andreev, D. Cline, R. Cousins, J. Duris, S. Erhan, P. Everaerts, C. Farrell, J. Hauser, M. Ignatenko, C. Jarvis, C. Plager, G. Rakness, P. Schlein[†], P. Traczyk, V. Valuev, M. Weber

University of California, Riverside, Riverside, USA

J. Babb, R. Clare, M.E. Dinardo, J. Ellison, J.W. Gary, F. Giordano, G. Hanson, G.Y. Jeng⁵⁰, H. Liu, O.R. Long, A. Luthra, H. Nguyen, S. Paramesvaran, J. Sturdy, S. Sumowidagdo, R. Wilken, S. Wimpenny

University of California, San Diego, La Jolla, USA

W. Andrews, J.G. Branson, G.B. Cerati, S. Cittolin, D. Evans, F. Golf, A. Holzner, R. Kelley, M. Lebourgeois, J. Letts, I. Macneill, B. Mangano, S. Padhi, C. Palmer, G. Petrucciani, M. Pieri, M. Sani, V. Sharma, S. Simon, E. Sudano, M. Tadel, Y. Tu, A. Vartak, S. Wasserbaech⁵¹, F. Würthwein, A. Yagil, J. Yoo

University of California, Santa Barbara, Santa Barbara, USA

D. Barge, R. Bellan, C. Campagnari, M. D'Alfonso, T. Danielson, K. Flowers, P. Geffert, J. Incandela, C. Justus, P. Kalavase, S.A. Koay, D. Kovalskyi, V. Krutelyov, S. Lowette, N. Mccoll, V. Pavlunin, F. Rebassoo, J. Ribnik, J. Richman, R. Rossin, D. Stuart, W. To, C. West

California Institute of Technology, Pasadena, USA

A. Apresyan, A. Bornheim, Y. Chen, E. Di Marco, J. Duarte, M. Gataullin, Y. Ma, A. Mott, H.B. Newman, C. Rogan, M. Spiropulu, V. Timciuc, J. Veverka, R. Wilkinson, S. Xie, Y. Yang, R.Y. Zhu

Carnegie Mellon University, Pittsburgh, USA

B. Akgun, V. Azzolini, A. Calamba, R. Carroll, T. Ferguson, Y. Iiyama, D.W. Jang, Y.F. Liu, M. Paulini, H. Vogel, I. Vorobiev

University of Colorado at Boulder, Boulder, USA

J.P. Cumalat, B.R. Drell, W.T. Ford, A. Gaz, E. Luiggi Lopez, J.G. Smith, K. Stenson, K.A. Ulmer, S.R. Wagner

Cornell University, Ithaca, USA

J. Alexander, A. Chatterjee, N. Eggert, L.K. Gibbons, B. Heltsley, A. Khukhunaishvili, B. Kreis, N. Mirman, G. Nicolas Kaufman, J.R. Patterson, A. Ryd, E. Salvati, W. Sun, W.D. Teo, J. Thom, J. Thompson, J. Tucker, J. Vaughan, Y. Weng, L. Winstrom, P. Wittich

Fairfield University, Fairfield, USA

D. Winn

Fermi National Accelerator Laboratory, Batavia, USA

S. Abdullin, M. Albrow, J. Anderson, L.A.T. Bauerdick, A. Beretvas, J. Berryhill, P.C. Bhat, I. Bloch, K. Burkett, J.N. Butler, V. Chetluru, H.W.K. Cheung, F. Chlebana, V.D. Elvira, I. Fisk, J. Freeman, Y. Gao, D. Green, O. Gutsche, J. Hanlon, R.M. Harris, J. Hirschauer, B. Hooberman, S. Jindariani, M. Johnson, U. Joshi, B. Kilminster, B. Klima, S. Kunori, S. Kwan, C. Leonidopoulos, J. Linacre, D. Lincoln, R. Lipton, J. Lykken, K. Maeshima, J.M. Marraffino, S. Maruyama, D. Mason, P. McBride, K. Mishra, S. Mrenna, Y. Musienko⁵², C. Newman-Holmes, V. O'Dell, O. Prokofyev, E. Sexton-Kennedy, S. Sharma, W.J. Spalding, L. Spiegel, L. Taylor, S. Tkaczyk, N.V. Tran, L. Uplegger, E.W. Vaandering, R. Vidal, J. Whitmore, W. Wu, F. Yang, F. Yumiceva, J.C. Yun

University of Florida, Gainesville, USA

D. Acosta, P. Avery, D. Bourilkov, M. Chen, T. Cheng, S. Das, M. De Gruttola, G.P. Di Giovanni, D. Dobur, A. Drozdetskiy, R.D. Field, M. Fisher, Y. Fu, I.K. Furic, J. Gartner, J. Hugon, B. Kim, J. Konigsberg, A. Korytov, A. Kropivnitskaya, T. Kypreos, J.F. Low, K. Matchev, P. Milenovic⁵³, G. Mitselmakher, L. Muniz, M. Park, R. Remington, A. Rinkevicius, P. Sellers, N. Skhirtladze, M. Snowball, J. Yelton, M. Zakaria

Florida International University, Miami, USA

V. Gaultney, S. Hewamanage, L.M. Lebolo, S. Linn, P. Markowitz, G. Martinez, J.L. Rodriguez

Florida State University, Tallahassee, USA

T. Adams, A. Askew, J. Bochenek, J. Chen, B. Diamond, S.V. Gleyzer, J. Haas, S. Hagopian, V. Hagopian, M. Jenkins, K.F. Johnson, H. Prosper, V. Veeraraghavan, M. Weinberg

Florida Institute of Technology, Melbourne, USA

M.M. Baarmand, B. Dorney, M. Hohlmann, H. Kalakhety, I. Vodopiyanov

University of Illinois at Chicago (UIC), Chicago, USA

M.R. Adams, I.M. Anghel, L. Apanasevich, Y. Bai, V.E. Bazterra, R.R. Betts, I. Bucinskaite, J. Callner, R. Cavanaugh, O. Evdokimov, L. Gauthier, C.E. Gerber, D.J. Hofman, S. Khalatyan, F. Lacroix, M. Malek, C. O'Brien, C. Silkworth, D. Strom, P. Turner, N. Varelas

The University of Iowa, Iowa City, USA

U. Akgun, E.A. Albayrak, B. Bilki⁵⁴, W. Clarida, F. Duru, J.-P. Merlo, H. Mermerkaya⁵⁵, A. Mestvirishvili, A. Moeller, J. Nachtman, C.R. Newsom, E. Norbeck, Y. Onel, F. Ozok⁵⁶, S. Sen, P. Tan, E. Tiras, J. Wetzel, T. Yetkin, K. Yi

Johns Hopkins University, Baltimore, USA

B.A. Barnett, B. Blumenfeld, S. Bolognesi, D. Fehling, G. Giurgiu, A.V. Gritsan, Z.J. Guo, G. Hu, P. Maksimovic, S. Rappoccio, M. Swartz, A. Whitbeck

The University of Kansas, Lawrence, USA

P. Baringer, A. Bean, G. Benelli, R.P. Kenny Iii, M. Murray, D. Noonan, S. Sanders, R. Stringer, G. Tinti, J.S. Wood, V. Zhukova

Kansas State University, Manhattan, USA

A.F. Barfuss, T. Bolton, I. Chakaberia, A. Ivanov, S. Khalil, M. Makouski, Y. Maravin, S. Shrestha, I. Svintradze

Lawrence Livermore National Laboratory, Livermore, USA

J. Gronberg, D. Lange, D. Wright

University of Maryland, College Park, USA

A. Baden, M. Boutemeur, B. Calvert, S.C. Eno, J.A. Gomez, N.J. Hadley, R.G. Kellogg, M. Kirn,

T. Kolberg, Y. Lu, M. Marionneau, A.C. Mignerey, K. Pedro, A. Peterman, A. Skuja, J. Temple, M.B. Tonjes, S.C. Tonwar, E. Twedt

Massachusetts Institute of Technology, Cambridge, USA

A. Apyan, G. Bauer, J. Bendavid, W. Busza, E. Butz, I.A. Cali, M. Chan, V. Dutta, G. Gomez Ceballos, M. Goncharov, K.A. Hahn, Y. Kim, M. Klute, K. Krajczar⁵⁷, P.D. Luckey, T. Ma, S. Nahn, C. Paus, D. Ralph, C. Roland, G. Roland, M. Rudolph, G.S.F. Stephans, F. Stöckli, K. Sumorok, K. Sung, D. Velicanu, E.A. Wenger, R. Wolf, B. Wyslouch, M. Yang, Y. Yilmaz, A.S. Yoon, M. Zanetti

University of Minnesota, Minneapolis, USA

S.I. Cooper, B. Dahmes, A. De Benedetti, G. Franzoni, A. Gude, S.C. Kao, K. Klapoetke, Y. Kubota, J. Mans, N. Pastika, R. Rusack, M. Sasseville, A. Singovsky, N. Tambe, J. Turkewitz

University of Mississippi, Oxford, USA

L.M. Cremaldi, R. Kroeger, L. Perera, R. Rahmat, D.A. Sanders

University of Nebraska-Lincoln, Lincoln, USA

E. Avdeeva, K. Bloom, S. Bose, J. Butt, D.R. Claes, A. Dominguez, M. Eads, J. Keller, I. Kravchenko, J. Lazo-Flores, H. Malbouisson, S. Malik, G.R. Snow

State University of New York at Buffalo, Buffalo, USA

A. Godshalk, I. Iashvili, S. Jain, A. Kharchilava, A. Kumar

Northeastern University, Boston, USA

G. Alverson, E. Barberis, D. Baumgartel, M. Chasco, J. Haley, D. Nash, D. Trocino, D. Wood, J. Zhang

Northwestern University, Evanston, USA

A. Anastassov, A. Kubik, N. Mucia, N. Odell, R.A. Ofierzynski, B. Pollack, A. Pozdnyakov, M. Schmitt, S. Stoynev, M. Velasco, S. Won

University of Notre Dame, Notre Dame, USA

L. Antonelli, D. Berry, A. Brinkerhoff, K.M. Chan, M. Hildreth, C. Jessop, D.J. Karmgard, J. Kolb, K. Lannon, W. Luo, S. Lynch, N. Marinelli, D.M. Morse, T. Pearson, M. Planer, R. Ruchti, J. Slaunwhite, N. Valls, M. Wayne, M. Wolf

The Ohio State University, Columbus, USA

B. Bylsma, L.S. Durkin, C. Hill, R. Hughes, K. Kotov, T.Y. Ling, D. Puigh, M. Rodenburg, C. Vuosalo, G. Williams, B.L. Winer

Princeton University, Princeton, USA

N. Adam, E. Berry, P. Elmer, D. Gerbaudo, V. Halyo, P. Hebda, J. Hegeman, A. Hunt, P. Jindal, D. Lopes Pegna, P. Lujan, D. Marlow, T. Medvedeva, M. Mooney, J. Olsen, P. Piroué, X. Quan, A. Raval, B. Safdi, H. Saka, D. Stickland, C. Tully, J.S. Werner, A. Zuranski

University of Puerto Rico, Mayaguez, USA

E. Brownson, A. Lopez, H. Mendez, J.E. Ramirez Vargas

Purdue University, West Lafayette, USA

E. Alagoz, V.E. Barnes, D. Benedetti, G. Bolla, D. Bortoletto, M. De Mattia, A. Everett, Z. Hu, M. Jones, O. Koybasi, M. Kress, A.T. Laasanen, N. Leonardo, V. Maroussov, P. Merkel, D.H. Miller, N. Neumeister, I. Shipsey, D. Silvers, A. Svyatkovskiy, M. Vidal Marono, H.D. Yoo, J. Zablocki, Y. Zheng

Purdue University Calumet, Hammond, USA

S. Guragain, N. Parashar

Rice University, Houston, USA

A. Adair, C. Boulahouache, K.M. Ecklund, F.J.M. Geurts, W. Li, B.P. Padley, R. Redjimi, J. Roberts, J. Zabel

University of Rochester, Rochester, USA

B. Betchart, A. Bodek, Y.S. Chung, R. Covarelli, P. de Barbaro, R. Demina, Y. Eshaq, T. Ferbel, A. Garcia-Bellido, P. Goldenzweig, J. Han, A. Harel, D.C. Miner, D. Vishnevskiy, M. Zielinski

The Rockefeller University, New York, USA

A. Bhatti, R. Ciesielski, L. Demortier, K. Goulios, G. Lungu, S. Malik, C. Mesropian

Rutgers, the State University of New Jersey, Piscataway, USA

S. Arora, A. Barker, J.P. Chou, C. Contreras-Campana, E. Contreras-Campana, D. Duggan, D. Ferencek, Y. Gershtein, R. Gray, E. Halkiadakis, D. Hidas, A. Lath, S. Panwalkar, M. Park, R. Patel, V. Rekovic, J. Robles, K. Rose, S. Salur, S. Schnetzer, C. Seitz, S. Somalwar, R. Stone, S. Thomas

University of Tennessee, Knoxville, USA

G. Cerizza, M. Hollingsworth, S. Spanier, Z.C. Yang, A. York

Texas A&M University, College Station, USA

R. Eusebi, W. Flanagan, J. Gilmore, T. Kamon⁵⁸, V. Khotilovich, R. Montalvo, I. Osipenkov, Y. Pakhotin, A. Perloff, J. Roe, A. Safonov, T. Sakuma, S. Sengupta, I. Suarez, A. Tatarinov, D. Toback

Texas Tech University, Lubbock, USA

N. Akchurin, J. Damgov, C. Dragoiu, P.R. Duderu, C. Jeong, K. Kovitanggoon, S.W. Lee, T. Libeiro, Y. Roh, I. Volobouev

Vanderbilt University, Nashville, USA

E. Appelt, A.G. Delannoy, C. Florez, S. Greene, A. Gurrola, W. Johns, P. Kurt, C. Maguire, A. Melo, M. Sharma, P. Sheldon, B. Snook, S. Tuo, J. Velkovska

University of Virginia, Charlottesville, USA

M.W. Arenton, M. Balazs, S. Boutle, B. Cox, B. Francis, J. Goodell, R. Hirosky, A. Ledovskoy, C. Lin, C. Neu, J. Wood

Wayne State University, Detroit, USA

S. Gollapinni, R. Harr, P.E. Karchin, C. Kottachchi Kankanamge Don, P. Lamichhane, A. Sakharov

University of Wisconsin, Madison, USA

M. Anderson, D. Belknap, L. Borrello, D. Carlsmith, M. Cepeda, S. Dasu, E. Friis, L. Gray, K.S. Grogg, M. Grothe, R. Hall-Wilton, M. Herndon, A. Hervé, P. Klabbers, J. Klukas, A. Lanaro, C. Lazaridis, J. Leonard, R. Loveless, A. Mohapatra, I. Ojalvo, F. Palmonari, G.A. Pierro, I. Ross, A. Savin, W.H. Smith, J. Swanson

†: Deceased

1: Also at Vienna University of Technology, Vienna, Austria

2: Also at National Institute of Chemical Physics and Biophysics, Tallinn, Estonia

3: Also at Universidade Federal do ABC, Santo Andre, Brazil

4: Also at California Institute of Technology, Pasadena, USA

- 5: Also at CERN, European Organization for Nuclear Research, Geneva, Switzerland
- 6: Also at Laboratoire Leprince-Ringuet, Ecole Polytechnique, IN2P3-CNRS, Palaiseau, France
- 7: Also at Suez Canal University, Suez, Egypt
- 8: Also at Zewail City of Science and Technology, Zewail, Egypt
- 9: Also at Cairo University, Cairo, Egypt
- 10: Also at Fayoum University, El-Fayoum, Egypt
- 11: Also at British University, Cairo, Egypt
- 12: Now at Ain Shams University, Cairo, Egypt
- 13: Also at National Centre for Nuclear Research, Swierk, Poland
- 14: Also at Université de Haute-Alsace, Mulhouse, France
- 15: Now at Joint Institute for Nuclear Research, Dubna, Russia
- 16: Also at Moscow State University, Moscow, Russia
- 17: Also at Brandenburg University of Technology, Cottbus, Germany
- 18: Also at Institute of Nuclear Research ATOMKI, Debrecen, Hungary
- 19: Also at Eötvös Loránd University, Budapest, Hungary
- 20: Also at Tata Institute of Fundamental Research - HECR, Mumbai, India
- 21: Also at University of Visva-Bharati, Santiniketan, India
- 22: Also at Sharif University of Technology, Tehran, Iran
- 23: Also at Isfahan University of Technology, Isfahan, Iran
- 24: Also at Plasma Physics Research Center, Science and Research Branch, Islamic Azad University, Tehran, Iran
- 25: Also at Facoltà Ingegneria Università di Roma, Roma, Italy
- 26: Also at Università della Basilicata, Potenza, Italy
- 27: Also at Università degli Studi Guglielmo Marconi, Roma, Italy
- 28: Also at Università degli Studi di Siena, Siena, Italy
- 29: Also at University of Bucharest, Faculty of Physics, Bucuresti-Magurele, Romania
- 30: Also at Faculty of Physics of University of Belgrade, Belgrade, Serbia
- 31: Also at University of California, Los Angeles, Los Angeles, USA
- 32: Also at Scuola Normale e Sezione dell' INFN, Pisa, Italy
- 33: Also at INFN Sezione di Roma; Università di Roma, Roma, Italy
- 34: Also at University of Athens, Athens, Greece
- 35: Also at Rutherford Appleton Laboratory, Didcot, United Kingdom
- 36: Also at The University of Kansas, Lawrence, USA
- 37: Also at Paul Scherrer Institut, Villigen, Switzerland
- 38: Also at Institute for Theoretical and Experimental Physics, Moscow, Russia
- 39: Also at Gaziosmanpasa University, Tokat, Turkey
- 40: Also at Adiyaman University, Adiyaman, Turkey
- 41: Also at Izmir Institute of Technology, Izmir, Turkey
- 42: Also at The University of Iowa, Iowa City, USA
- 43: Also at Mersin University, Mersin, Turkey
- 44: Also at Ozyegin University, Istanbul, Turkey
- 45: Also at Kafkas University, Kars, Turkey
- 46: Also at Suleyman Demirel University, Isparta, Turkey
- 47: Also at Ege University, Izmir, Turkey
- 48: Also at School of Physics and Astronomy, University of Southampton, Southampton, United Kingdom
- 49: Also at INFN Sezione di Perugia; Università di Perugia, Perugia, Italy
- 50: Also at University of Sydney, Sydney, Australia
- 51: Also at Utah Valley University, Orem, USA

52: Also at Institute for Nuclear Research, Moscow, Russia

53: Also at University of Belgrade, Faculty of Physics and Vinca Institute of Nuclear Sciences, Belgrade, Serbia

54: Also at Argonne National Laboratory, Argonne, USA

55: Also at Erzincan University, Erzincan, Turkey

56: Also at Mimar Sinan University, Istanbul, Istanbul, Turkey

57: Also at KFKI Research Institute for Particle and Nuclear Physics, Budapest, Hungary

58: Also at Kyungpook National University, Daegu, Korea